FE200614

NTIS
One Source. One Search. One Solution.

APPLIED RESEARCH AND EVALUATION OF PROCESS CONCEPTS FOR LIQUEFACTION AND GASIFICATION OF WESTERN COALS. QUARTERLY PROGRESS REPORT, OCTOBER-DECEMBER 1978

UTAH UNIV., SALT LAKE CITY. DEPT. OF
MINING AND FUELS ENGINEERING

MAR 1979

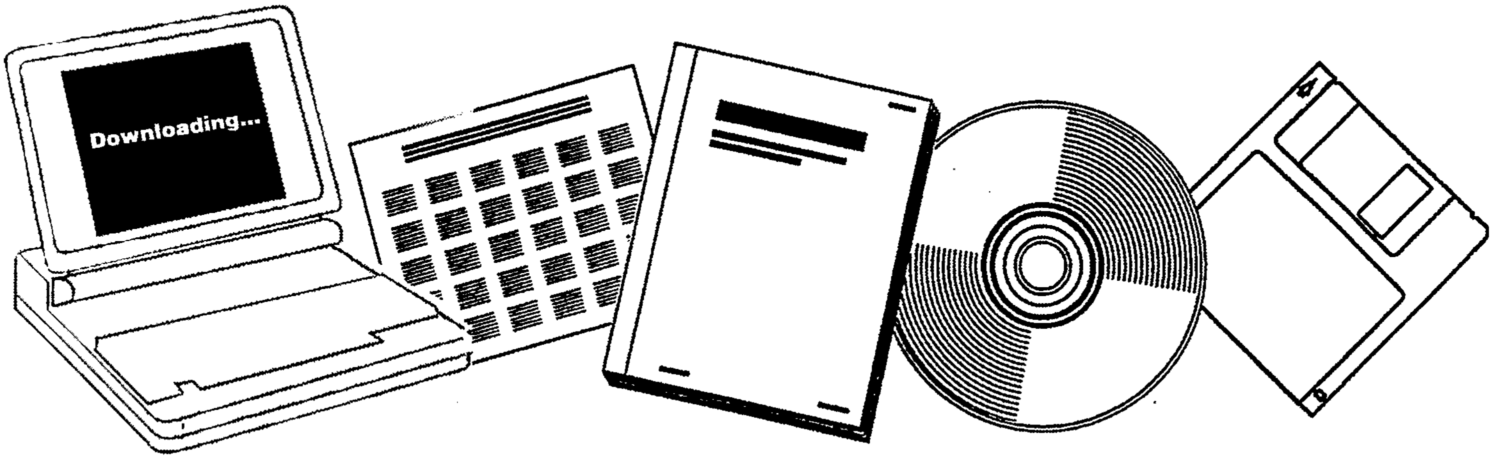

U.S. Department of Commerce
National Technical Information Service

One Source. One Search. One Solution.

NTIS

Providing Permanent, Easy Access to U.S. Government Information

National Technical Information Service is the nation's largest repository and disseminator of government-initiated scientific, technical, engineering, and related business information. The NTIS collection includes almost 3,000,000 information products in a variety of formats: electronic download, online access, CD-ROM, magnetic tape, diskette, multimedia, microfiche and paper.

Search the NTIS Database from 1990 forward

NTIS has upgraded its bibliographic database system and has made all entries since 1990 searchable on **www.ntis.gov.** You now have access to information on more than 600,000 government research information products from this web site.

Link to Full Text Documents at Government Web Sites

Because many Government agencies have their most recent reports available on their own web site, we have added links directly to these reports. When available, you will see a link on the right side of the bibliographic screen.

Download Publications (1997 - Present)

NTIS can now provides the full text of reports as downloadable PDF files. This means that when an agency stops maintaining a report on the web, NTIS will offer a downloadable version. There is a nominal fee for each download for most publications.

For more information visit our website:

www.ntis.gov

U.S. DEPARTMENT OF COMMERCE
Technology Administration
National Technical Information Service
Springfield, VA 22161

023067

FE200614

FE-2006-14
Dist Category UC-90

Applied Research and Evaluation of Process Concepts for Liquefaction and Gasification of Western Coals

Quarterly Progress Report
for the Period Oct - Dec 1978

Dr. Wendell H. Wiser

University of Utah - Department
of Mining and Fuels Engineering
Salt Lake City, Utah 84112

Date Published - March 1979

Prepared for the United States
Department of Energy

Under Contract No. E(49-18) - 2006

REPRODUCED BY
NATIONAL TECHNICAL
INFORMATION SERVICE
U.S. DEPARTMENT OF COMMERCE
SPRINGFIELD, VA. 22161

NOTICE

This report was prepared as an account of work sponsored by the United States Government. Neither the United States nor the United States Department of Energy, nor any of their employees, makes any warranty, express or implied, or assumes any legal liability or responsibility for the accuracy, completeness, or usefulness of any information, apparatus, product, or process disclosed, or represents that its use would not infringe privately owned rights. Reference herein to any specific commercial product, process, or service by trade name, mark, manufacturer, or otherwise, does not necessarily constitute or imply its endorsement, recommendation, or favoring by the United States Government or any agency thereof. The views and opinions of authors expressed herein do not necessarily state or reflect those of the United States Government or any agency thereof.

Available from:

National Technical Information Service (NTIS)
U.S. Department of Commerce
5285 Port Royal Road
Springfield, Virginia 22161

Price: Printed copy: $6.00
Microfiche: $3.00

CONTENTS

II. OBJECTIVE AND SCOPE OF WORK

The research reported herein is all of fundamental importance in support of either a process for development of liquefaction of coal, catalysis or some related research. The information which will be gained by research on this contract should materially assist the application of coal in the solution of the energy problems now facing the United States and the world. In particular, the projects reported herein are intended to apply the expertise developed by the coal research team at the University of Utah to problems in four general areas:

a) Evaluation of process concepts in relation to liquefaction and gasification of coal,
b) Catalysis studies of fundamental importance in liquefaction and gasification of coal,
c) Studies of fundamental principles involved in processes for liquefaction and gasification of coal,
d) Properties of coal and coal conversion products of significance in liquefaction and gasification of coal.

A-1 Coal will be gasified by direct catalytic hydrogenation to produce a high-BTU gas. A liquid will be produced in a first stage reaction at 400-450°C. This product will be further hydrogenated to produce a high-BTU gas. Catalysts and reaction conditions for each stage will be studied.

A-2 Kinetics, yields and optimum reaction conditions for extraction of coal will be determined. Hydrogen donor solvents, ultrasonic energy, hydrogen pressures and catalysts will be employed. Extraction products will be analyzed and characterized.

A-4 Aromatic liquids derived from coal hydrogenation or extraction will be considered as feedstocks for steam reforming to make a high-BTU gas. Optimum conditions for the production of hydrogen or high-BTU gas, optimum catalysts, the effects of poisons and the degree of coke formation will be determined.

A-6 The gasification of coal char will be studied at 2000-3000 psi to produce hydrogen for coal hydrogenation. Steam and oxygen will be used for gasification. The thermal efficiency of producing hydrogen at the pressure at which it will be used will be studied.

A-7 Thermal hydrogenolysis of coal slurried with recycle solvent will be studied as such or in the presence of a vapor-phase catalyst to determine the extent of upgrading.

A-8 Fischer-Tropsch synthesis of C_2-C_4 hydrocarbons will be studied. New catalysts will be developed and a continuous test unit for long-term catalyst testing will be constructed.

A-9 The capacity and durability of a previously developed high-pressure gas recycle pump will be increased. A goal of 3000 psi operating pressure at 500°C is desirable.

B-1 Adsorption properties and penetration of aromatic molecules on typical cracking catalysts will be determined. These properties will be used to evaluate the ability of such catalysts to crack the large molecules present in coal-derived liquids.

B-2 (alternate) The mechanism of deactivation of molybdena hydrodesulfurization catalysts by coal-derived liquids will be studied. Kinetic studies involving the model compound benzothiophene will be employed.

B-3 Hydrogen transfer by metal halide catalysts during coal hydrogenation will be studied. Deuterium labled hydrocarbons will be used to elucidate reaction mechanisms.

B-4 The mechanism of catalytic hydrogenation of coal by metal halide catalysts will be investigated. The nature of active catalyst sight will be studied. Changes in properties of the reacting coal will be determined and the nature of reaction products will be determined. Catalyst regeneration will also be studied.

C-1 The mechanism of pyrolysis of coal will be studied by the use of isotopically labled model compounds. Products of pyrolysis will be examined to determine their precursors in coal.

C-2 Fluid mechanics and heat transfer studies involving gas-solid suspensions in vertical downward cocurrent flow systems will be conducted to obtain information on the effect of these variables in the University ot Utah coal hydrogenation reactor.

D-1 The effect of coal and catalyst properties and pretreatment on the hydrogenation of western coals will be studied in the University of Utah short-residence-time, entrained-flow reactor.

D-2 The effect of coal structure on reactivity to hydrogenation, pyrolysis and dissolution will be studied. Pretreatment of the coal by specific reactions will be used to obtain samples with special structural features.

D-4 Liquid products from coal hydrogenation in the University of Utah reactor will be separated and characterized. Coal pyrolysis and hydrogenation mechanisms and model compound reactions will be studied.

III Summary of Progress to Date

Research Highlights

Students working on Projects A-4 and D-2 have completed their degree work.

Steam reforming of aromatic compounds has shown that dealkylation is faster than ring breakdown. Isomerization and polymerization does not occur. The rate of dealkylation and dehydrogenation decreases with increasing temperature and pressure. Reactivity decreases as the number of aromatic rings in the molecule increases.

Coal asphaltenes were shown to contain considerable amounts of hydroaromatic structures which can be dehydrogenated. They also contain acid-base structures which are dissociated by reaction with HCl.

Publications, Presentations and Activities

C. Russell, J. Shabtai, L. Veluswamy and A.G. Oblad, "Hydrogenation of Model Polycyclic Aromatics over Sulfided Catalysts," presented at the California Catalysis Soc., Oct 26, 1978, Laguna Beach, Calif.

S. Yokoyama, N. Tuzuki, T. Katoh, Y. Sanada, D.M. Bodily and Wendell H. Wiser, "Chemical Structure of Heavy Oil Derived from Coal Hydrogenation by Mass Spectroscopy," J. Fuel Soc., Japan, 5, 748 (1978).

F.E. Massoth, "Comments on 'Stabilization Effect of Co for Mo Phase in Co-Mo/Al_2O_3 Hydrodesulfurization Catalysts Studied with X-Ray Photoelectron Spectroscopy,'" J. Catal., 54, 450 (1978).

Project A-2

Solvent Treatment of Coal-Derived Liquids (CDL)

Faculty Advisor: L.L. Anderson
Graduate Student: Kwang Eun Chung

Introduction

The objective of this investigation is to separate CDL into chemically different fractions of potential commercial value. Major developments have included (1) the isolation of paraffinic material, (2) the separation of CDL into highly H-bonded and less H-bonded fractions, (3) the observation of free -OH bonds in the infrared spectra of CDL fractions in dilute solutions, (4) a new activity expression in liquid solutions and (5) a new procedure for molecular weight determination by vapor phase osmometry. Currently a new characterization scheme for CDL is being developed.

Project Status

A high volatile bituminous coal was solubilized by means of hydrolysis. The coal was the same as that from which the CDL was produced. However, the chemical characteristics of the two portions are not necessarily identical due to the different sampling procedures. The results on the solubilized coal are from one experiment and a duplicate run is in progress.

The hydrolysis was performed using procedures similar to that of Makabe.[1] Twenty-four grams of coal (-200 mesh) were solubilized at 320°C for 100 min. The product was divided into four fractions. The first two fractions, Fractions A and B, were soluble in a strong basic solution. When an acidic solution was added for neutralization, Fraction A precipitated as fine particles while Fraction B formed small lumps. The rest of the product was extracted at room temperature with pyridine to obtain Fraction C and an insoluble portion.

The four fractions were analyzed for elemental composition, molecular weight and/or structural parameters. Oxygen contents were determined by direct measurements. Molecular weights were obtained by a procedure previously reported using pyridine at 85°C.[2] Proton NMR spectra were obtained in pyridine-D_5 solutions. The analytical data except for the structural parameters are shown in Table 1.

The total product recovery amounted to 83% of the coal (MAF). The loss, 17% of coal, was due to the unrecovered material in the neutralized solution and gaseous product. Most of the recovered product, 92%, was in the soluble fractions. The high yield of the product and its good solubility indicate that the soluble fractions A, B and C represent a major portion of the carbonaceous material in coal.

The data in the Tables may be useful in accessing the nature of coal. In this report, however, the data were analyzed in relation to the information drawn from the characterization of CDL-P in the last report. The CDL-P represented approximately 70% of the liquid and solid product, with the other 30% being char, paraffinic material and light hydrocarbons (BP < 150°C) produced in the University of Utah hydrogenation reactor. The condensed phase product amounted to 75% of coal (MAF) with the rest being water and gases. Thus CDL-P is a major fraction of coal and may retain information on the skeletal aspects of coal. However, CDL-P underwent more severe processing conditions than the solubilization product, and it is interesting to compare their structural characteristics.

Structural parameters of the solubilization product were calculated by the same procedure described in the last report and are shown in Table 2 along with those of CDL-P. The molecular weights of the three fractions of the solubilization product are almost twice that of CDL-P. Considering the milder processing conditions and specificity of the hydrolysis reaction, the solubilization product is expected to retain more structural characteristics of coal than CDL-P.

Before making a comparison to CDL-P, it is beneficial to examine the characteristics of the solubilization product. Molecular weights, number of naphthenic rings (R_N), aromaticity (f_a) and number of oxygen per molecule (#O) are similar in the three fractions.

The significant differences are the number of aromatic rings (R_A) and aromatic clusters (#Cl). Fraction C has the largest R_A, but the smallest #Cl. Fractions A and B have smaller R_A but larger #Cl. Since a larger #Cl indicates that more aromatic clusters are separated by saturated bonds, the molecules in Fractions A and B could be cleaved to obtain substantially smaller species. However Fraction C consists of molecules all having nearly one aromatic cluster. Therefore, there are two major component groups in the solubilized product. One group has a smaller R_A, yet is reducible to smaller molecules, while the other group has a larger R_A and is difficult to reduce to smaller molecules.

On comparison the solubilization product has larger structural parameters than CDL-P except for f_a. The larger parameters are related to molecular size, skeletal structure and possible linkages. These results were expected due to the milder processing conditions and the specificity of the hydrolysis reaction. The solubilization product may be an intermediate for CDL-P and could possibly be converted to CDL-P under conditions that yield CDL-P.

The structural parameters, R_A and #Cl, suggest that cleaving saturated bonds between aromatic clusters in Fractions A and B will result in "light," "middle" or "heavy." Fractions A and B will not become "resid" by this cleavage. Fraction C, however, cannot be converted to "light," "middle" or "heavy," but becomes "resid."

The above conversion of the three fractions to CDL-P fractions may be accompanied by a small increase in aromaticity, f_a, in spite of the large decreases in the other parameters. Any increase in f_a is attributable to preferential disappearance of aliphatic carbons by evolution of gases or conversion of aliphatic carbons to aromatic carbons. The evolution of a small amount of C_1-C_6 gases when producing CDL, and the removal of paraffinic material when preparing CDL-P, may cause the slight change in f_a implying that there have been no major alterations to the skeleton and minimal changes of aliphatic to aromatic carbon in the conversion process.

Theoretically a pseudo-predecessor of CDL-P should retain most of the structural features of the true predecessor that could survive the processing conditions. Structural parameters for the pseudo-predecessor,"pred," in Table 2 were calculated as the following: (1) its molecular weight and aromaticity were taken as the same as those of the solubilization product, (2) others except #Cl were computed from those of CDL-P assuming that the magnitude of each parameter was proportional to molecular weight, and (3) the value of #Cl was estimated and will be discussed in the next report..

Since a true predecessor was not available, the pseudo-predecessor was compared with the solubilization product, which may be an intermediate for CDL-P as discussed previously. Two parameters, R_A and #Cl, in "pred" were slightly larger than those in the solubilized product, while R_N and #O were appreciably smaller. The small differences in the former two parameters suggest that they are essentially unchanged and may be caused by variations in coal sampling, yields and processing conditions when obtaining the solubilization product and CDL-P.

The appreciable decrease in R_N and #O deserves careful attention because they may relate to weak bonds or linkages in coal and its derivatives. The decreases are 42% for R_N and 47% for #O, and were accompanied by a large reduction in molecular weight from 485 to 268. The molecular weight reduction requires the breakage of approximately one linkage in 80% of the average molecules. A decrease in both the parameters is therefore important. Since the reduction in the molecular weight is the major cause of liquefaction of coal, further understanding of the roles of two parameters is sought.

In the last report it was postulated that methyl groups α to aromatic rings, $(-CH_3)_\alpha$, in CDL-P could be vestigial remains of $(-CH_2-)_n$ linkages. In the three fractions of the solubilization product, α-methyl groups do not appear in any significant quantity. This observation supports the relationship between $(-CH_3)_\alpha$ in CDL-P and $(-CH_2-)_n$ in coal. The appearance of $(-CH_3)_\alpha$ will be further examined.

Future Work

Further interpretation and experimentation using the new characterization scheme will be performed.

References

1. M. Makabe et al., Fuel, 57, 289 (1978).

2. W. H. Wiser et al., ERDA No.(49-18)-2006, Quarterly Progress Report, Salt Lake City, Utah, Oct-Dec 1977, p 14.

Table 1. Analytical Data on the Coal and Its Solubilization Product.

	Yield,%	C%	H%	N%	O%	Δ%[a]
Coal (MAF)	100	76.1	5.0	1.4	17.9	-0.4
Fraction A	26.6	72.6	6.9	1.0	7.7	11.8
B	23.8	71.7	7.6	1.0	8.5	11.2
C	26.1	80.5	8.1	1.4	6.8	3.2
Insoluble	6.4[b]	14.7	1.3	0.1	22.6	61.3

---

[a] Δ% = 100 - C% - H% - N% - O%

[b] Ash content not included, which is 75% of Insoluble.

Table 2. Structural Parameters for the Solubilization Product and CDL-P.

	Yield[a]	Mol. Wt.	R_A	R_N	#Cl[b]	f_a	#O[b]
Solub. Product[c]	76.5	485	3.2	2.4	1.3	0.50	2.32
Fraction A	26.6	478	3.2	2.5	1.4	0.54	2.31
B	23.8	444	2.4	2.3	1.3	0.47	2.36
C	26.1	538	4.0	2.3	1.1	0.50	2.27
CDL-P[c]	46.2	268	2.4	0.9	1.1	0.60	0.77
Light	9.6	183	1.2	0.6	1.0	0.55	0.63
Middle	7.8	210	1.6	0.7	1.1	0.58	0.67
Heavy	8.8	272	2.4	1.3	1.1	0.59	0.75
Resid	20.0	396	4.4	1.2	1.3	0.68	1.01
Pred.[d]		485	3.6	1.4	∿1.5	0.50	1.2

---

[a] Weight % of coal (MAF).

[b] Number of aromatic clusters, and number of oxygen/molecule, resp.

[c] The parameters are calculated from those of respective fractions.

[d] Pseudo-predecessor of CDL-P (See text).

Project A-2

A Systematic Study of Coal Structure by Extraction Liquefaction Under Mild Reaction Conditions

Faculty Advisor: J. Shabtai
Graduate Student: H.B. Oblad

Introduction

This study is concerned with extractive coal liquefaction under mild experimental conditions, using a variety of solvents and homogeneous catalysts. Coal slurries will be processed in a small integral flow reactor which will be operated at temperatures of 100-300°C, hydrogen pressures of 100-1000 psig and very short residence times. The mild conditions will be adjusted to obtain very low coal conversions, e.g., 2-5 percent to avoid secondary reactions. The slurry will be quenched, the liquids will be removed and analyzed, and the washed solids will be reloaded into the reactor with fresh solvent and catalyst. Repetition of this procedure coupled with the application of selective catalysts should yield relatively simple primary products. The information gathered should reveal the types of original structural components and interconnecting functional groups present in coal.

Project Status

Preliminary coal extraction experiments are being performed to clarify the action of solvents and reaction conditions on the raw coal. It is essential to be able to differentiate the true products of reaction from those mobilized by simple solvation. A sequence of extensive washings is being performed on coal and spectrometric characterization will be done on the extracts.

A more suitable method for sequential extraction of the coal has been developed. Soxhlet extraction was also tried but was unsatisfactory. A simpler, more reliable method using multiple washings in large centrifuge tubes has been developed. A large centrifuge capable of holding 100 ml tubes was acquired but it was necessary to fabricate the tubes in this laboratory. Coal was weighed into 4 tubes (approx 9 g each) and 75 ml of solvent was added. The tubes were placed in a room temperature ultrasonic bath of deionized water and agitated for one hour. It was necessary to rotate the tubes every 15 minutes to ensure eveness of exposure to sound energy. The tubes were then spun (about 2300 rpm) in the large centrifuge for approximately one hour to settle the extremely fine suspension indicated by a crystal clear liquid phase.

The liquid was decanted and the solvent removed in a rotary evaporator. The accumulated residue was transferred using dichloromethane into a small tared vial, and the volatile solvent was blown off with a small stream of nitrogen. When dry the sample and vial were weighed and stored for spectrographic analysis. Thus far, Hiawatha, Utah coal has been extracted 7 times with cyclohexane and once with benzene. This method of extraction minimizes the handling of the coal and extract and results in superior material balances.

Future Work

Further extractions will be performed with solvents of increasing strength and the isolated extracts will be analyzed by IR and NMR spectrometry. A Kentucky coal will also undergo sequential washings and similar analyses.

Project A-4

Steam Reforming of Aromatic Compounds

Faculty Advisor: A.G. Oblad
Graduate Student: Shri Goyal

Introduction

The objective of this research is (1) to study the thermodynamics and kinetics of steam reforming and (2) to develop an appropriate catalyst for the steam reforming of aromatic compounds. The general reforming process and details of the equipment have been previously reported.

Project Status

The results obtained from the study of the steam reforming of aromatic compounds indicate the following:

1. Thermodynamic results suggest that the steam reforming of aromatic compounds can be carried out with slightly higher minimum steam ratios compared with that for methane and naphtha.

2. The most active catalyst which requires a minimum steam ratio for the steam reforming of aromatic compounds was the sodium promoted nickel catalyst having a composition of 71.4% Al_2O_3, 21.9% Ni and 6.70% Na (as Na_2O) on a wt basis.

3. The rate of reaction of benzene and steam over the above mentioned catalyst is first order with respect to benzene with an activation energy of 38.35 Kcal/mole, and the frequency factor is temperature dependent ($k_0 = aT^{3.5}$).

4. The primary products from the aromatic compounds-steam reaction are hydrogen and carbon dioxide.

5. The rate of dealkylation of alkyl-benzenes is faster than the rate of ring breakdown.

6. In the steam reforming of aromatic compounds, isomerization and polymerization does not take place.

7. The rate of dealkylation decreases with increased temperature and pressure.

8. The dehydrogenation of higher alkyl benzenes increases with increased temperature and decreases with increased pressure.

9. The reaction rate of alkyl benzenes decreases with the number of carbons in the side chain.

10. The reactivity of aromatic ring compounds decreases as the number of rings in the compound increases.

Future Work

This student has completed his thesis. The project will continue when a new student has been selected.

Project A-7

Catalytic Hydrodeoxygenation of Coal-Derived Liquids and Related Oxygen-Containing Compounds

Faculty Advisor: J. Shabtai
A.G. Oblad
Graduate Student: G. Haider

Introduction

Coal-derived liquids contain a high proportion of oxygen-containing compounds. Therefore, a systematic catalytic hydrodeoxygenation study of coal-derived liquids and related model compounds is being carried out. The study provides also information concerning the role of oxygen-containing compounds in coal liquefaction.

Project Status

Hydrodeoxygenation experiments were carried out with 1,4 benzodioxane and diphenyl ether. The intermediate products of noneliminating hydrogenolysis as well as the final products resulting from hydrodeoxygenation are being identified.

Future Work

The systematic hydrodeoxygenation studies of coal liquids and related oxygen-containing compounds will be continued.

Project A-7

Catalytic Cracking of Hydrogenated Coal Liquids and Related Polycyclic Naphthenes

Faculty Advisor: A.G. Oblad
J. Shabtai
Graduate Student: S. Sunder

Introduction

Hydrogenation followed by catalytic cracking provides a feasible process sequence for conversion of coal liquids into conventional fuels. Such a sequence has certain advantages in comparison with a hydrocracking catalytic reforming scheme.[1]

The present project is concerned with the following interrelated subjects:

(1) Systematic catalytic cracking studies of model polycyclic naphthenes found in hydrogenated coal liquids, e.g., decalin, perhydrophenanthrene and perhydroanthracene, as a function of catalyst type and operating conditions.

(2) Systematic catalytic cracking studies of hydrogenated coal-derived liquids (hydro-CDL) as a function of the same variables.

Catalysts applied in the study include both conventional zeolite-containing systems, e.g., Mobil Durabead, as well as newly developed large pore molecular sieves. The latter are prepared by cross-linking of layer silicates and are designated as CLS catalysts.[2,3] Strongly acidic H-forms of CLS are being tested as cracking catalysts. Such H-CDL systems have an important advantage over conventional zeolites in possessing sufficiently large pore sizes, e.g., 10-20 Å, for admission of polycyclic naphthenes in the catalyst intracrystalline channel system.

The equipment used and the methods of identification of products have been previously reported.

Project Status

The types of products obtained by cracking decalin and perhydrophenanthrene have been described in previous reports. During this quarter decalin has been studied in more detail.

The effect of temperature between 300-450°C and the space velocity between 0.80 and 5.0 g decalin per g catalyst were determined. The products were separated into coke, gas and liquid fractions. The gas and liquid fractions were analyzed by gas chromatography. A computer program has been made to convert the GC output to product distribution as a function of weight percent of decalin converted. However, identification of liquid products by mass spectrometry is still pending due to equipment failure at the College of Pharmacy.

Future Work

Perhydrophenanthrene and hydrogenated coal liquids will be studied in detail.

References

1. L.R. Veluswamy, Ph.D. Thesis, University of Utah, Salt Lake City, Utah, 1977.

2. J. Shabtai and N. Lahav, Israel Patent 50548; U.S. Patent pending.

3. N. Lahav, V. Shani and J. Shabtai, Clays and Clay Minerals, 26 (2), 107-115 (1978).

Project A-7

Catalytic Cracking of Coal-Derived Liquids

Faculty Advisor: F.V. Hanson
Graduate Student: Jay Dorius

Introduction

The catalytic cracking of coal-derived liquids may provide a viable means of upgrading these liquids to a marketable product. Previous studies have demonstrated that short residence time, high temperature fluid catalytic cracking of petroleum derived heavy gas oils to fuel oil and/or gasoline is feasible. The objective of the present investigation is to extend this work to coal-derived liquids.

Project Status

Initial testing and experiments are being carried out at the present time. These experiments are being conducted using a heavy virgin gas oil feedstock and a typical zeolite cracking catalyst. The purpose of these experiments is to shake down the equipment, solve the problems which exist, and formulate start-up and operating procedures. A block diagram of the system is shown in Figure 1.

Future Work

A reference set of experiments will be conducted to provide a benchmark for the study of the catalytic cracking of coal-derived liquids. These experiments will be carried out using a variety of cracking feedstocks, including those derived from paraffinic and naphthenic crudes.

The reference experiments will be conducted at temperatures from 723 - 873°K, catalyst to oil ratios of 2-5 wt/wt, and at atmospheric pressure. Feedstocks for subsequent experiments will consist of coal-derived liquids (5-25%) blended with typical catalytic cracking feedstocks. The coal-derived liquids will be obtained from subbituminous coal, a high volatile bituminous coal and a medium volatile bituminous coal. Commercially available amorphous (high pore volume, low and high alumina silica-aluminas) and crystalline (zeolite) catalysts will be utilized for this work.

A-Feed Reservoir
B-Feed Preheater
C-Catalyst Regenerator-Hopper
D-Riser Reactor
E-Pressure Gauge
F-Vapor-Solid Separation System Consists of a Disengager Tube and Cyclone Separator
G-Catalyst Receiving Vessel
H-Condenser
I-Liquid Product Collector
J-Gas Scrubber
K-Gas Flow Meter
L-Air Compressor
M-Metering Valves
N-Rotometer
O-Air Preheater
P-Feed Pump
Q-Nitrogen Supply
R-Regulator
S-Solids Metering Valve
T-Thermocouple
V-Valve

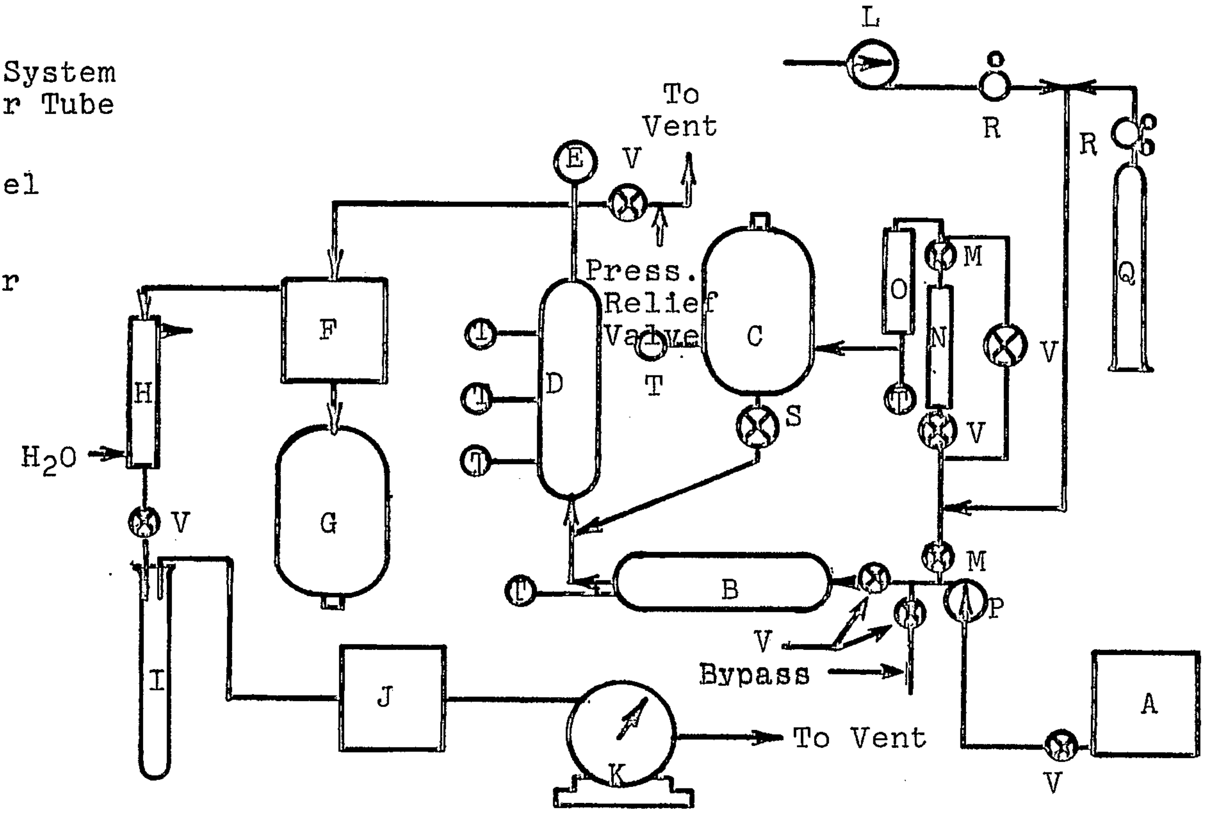

Figure 1. Diagram of Reaction System.

Page Intentionally Left Blank

Project A-8

Synthesis of Light Hydrocarbons From CO and H_2 (Continued)

Catalyst Characterization Studies

Faculty Advisor: F.E. Massoth
Graduate Student: K.B. Jensen

Introduction

This phase of the project is intended to supplement the high pressure reactor studies by detailed examination of the catalyst properties which enhance catalyst activity and selectivity. This is accomplished by characterization studies performed on the same catalysts which have been run in the reactor. Of particular interest are metal areas, evidence for alloy formation, phase structures and catalyst stability. Also, variables in catalyst preparation and pretreatment are examined to establish effects on catalyst properties. Finally, in-situ adsorption and activity are studied under modified reaction conditions with a number of well-characterized catalysts to obtain correlating relationships.

Previous characterization work was devoted to the copper-cobalt-alumina catalyst system. This study has been completed, and a Master's Degree Thesis has been written summarizing the findings.[1] A study has been initiated for characterizing iron-based catalysts. The latter catalysts have shown significant improvements in production of light olefins over that achieved by the Co-Cu-Al_2O_3 catalyst.[2] Characterization techniques similar to those developed for studying the Co-Cu-Al_2O_3 catalyst are being applied to the iron-based catalysts.

Project Status

Work has commenced on the characterization of iron-based catalysts. A literature survey of similar and related studies has been started and is continuing. Preliminary reduction and oxidation studies as well as some chemisorption studies have been performed using a flow microbalance system. X-Ray diffraction has been used to help identify bulk phases present in the reduced catalyst. The equipment presently in use is a Cahn Electrobalance with a catalyst sample bucket suspended in a quartz tube reactor at atmospheric pressure. The assembly is enclosed by an electric furnace and the temperature is monitored by a thermocouple well just below the catalyst bucket. A variety of atmospheres can be introduced into the reactor. Changes in weight of the catalyst sample during reduction or oxidation or during chemisorption are continuously monitored with a recorder readout. The X-ray diffraction unit is a Phillips Norelco machine using a goniometer. The sample is carefully powdered and placed in a shallow sample holder which is slipped into position for bombardment by the X-ray beam. Copper-K_α radiation is used.

High pressure reactor studies have shown that manganese-promoted unsupported iron catalysts gave marked improvements in C_2-C_4 selectivity and the olefin to paraffin ratio.[2] Initial characterization studies are consequently being performed on this catalyst system. Three representative catalysts have been chosen for this effort, viz., (1) the Fe base catalyst without Mn, (2) one containing a small amount of Mn and (3) one with a large amount of Mn. These catalysts had been prepared by a coprecipitation technique, the precipitating agent being ammonium carbonate for the former catalyst and ammonium hydroxide for the other two. The precipitates were oven dried overnight at 110°C. Compositions are given in Table 1.

The reduction characteristics of the catalysts were followed by the microbalance during heat-up to 500°C in a H_2 stream. Heating rates were only approximately linear in these initial screening runs. In general, four stages of weight loss were observed as shown in Figure 1. In the first only a small loss in weight was obtained up to about 200°C. The second stage gave a large, rapid weight loss in a rather small temperature range, except for Catalyst 44. This is most likely due to volatilization and decomposition of water, carbonate and/or nitrate. In the next stage, very little weight loss occurred over the next 200°C. The last stage again gave a rapid weight loss. This occurred between 400-500°C and was due to reduction of the iron oxide and possibly manganese oxide to lower valence states. After the final weight loss, the catalyst weight stabilized. The catalyst was left in H_2 at 500°C for about 20 hr to match the pretreatment procedure followed in the reactor studies.

After the reduction period, the catalyst was allowed to cool to room temperature and oxygen chemisorption was measured. Following this, the catalyst was reheated to 500°C in H_2 to remove the chemisorbed oxygen, then again cooled to room temperature to measure the CO chemisorption. Data are presented in Table 1. Values of O_2 adsorption are somewhat higher than CO adsorption. There are a number of possible reasons for this: (1) different adsorption stoichiometry, (2) additional bulk oxidation with O_2, (3) incomplete surface coverage with CO and (4) the effect of the presence of MnO (infra vide). With respect to the latter, it is informative to compare adsorption on a reduced iron basis. The results, given in Table 1, show an increase in O_2 adsorption with increased MnO content, whereas CO adsorption remains constant. The oxygen may adsorb on the MnO phase but not CO. This finding needs further corroboration, but if true, it can provide a means of determining the surface area of the individual phases present. For the iron only catalyst, a surface area of about 20 m^2/g (reduced catalyst) is calculated, assuming one O atom adsorbs per Fe site.

X-Ray diffraction studies were made on both the reduced and unreduced catalyst samples. The unreduced samples yielded data of limited value and were generally quite amorphous in their oven-dried state. However, the reduced sample gave clear spectra and valuable information concerning the bulk phases present in the catalyst. The X-ray diffraction pattern of Catalyst 4 yielded peaks whose position and intensity corresponded to the accepted values of α-iron. Catalysts 44 and 76 showed lines that corresponded to manganese oxide (MnO) in addition to the peaks corresponding to metallic iron. Iron and manganese metals have very simialr structure and lattice spacing so some manganese metal may be present in the reduced iron; however, spectra corresponding to MnO was found in Catalyst 44 and was even stronger in 76. A corollary experiment was performed on MnO by heating it in H_2 at 500°C for 20 hr. The resulting material had an X-ray pattern corresponding to accepted spectra for MnO and also matched the peaks and intensities found in the catalyst samples. No Mn metal phase was found in the X-ray pattern of this sample, signifying that MnO reduction under pretreatment conditions is negligible.

From the X-ray diffraction data of the catalysts, two phases appear to be present, Fe and MnO. However, because of similar structure and lattice spacing, a small amount of Mn metal might be present in the iron phase and some FeO in the MnO phase. Both Fe and Mn and FeO and MnO form solid solutions. X-Ray diffraction appears to be a very useful technique for bulk catalysts of this type, although it yields data valid only for the bulk properties of the catalyst. Surface oxides or metal determination will require additional techniques.

Future Work

Most of the work reported has been of a preliminary nature to gain an initial understanding of the catalyst phases present. A refined microbalance system of higher gas purity is being assembled to yield more conclusive chemisorption data. Pure MnO will be investigated to determine its adsorption properties. The BET surface areas of the catalysts will be measured to relate to the chemisorption studies. The mixed catalysts will be examined by electron microprobe to determine catalyst homogeneity. Future studies will involve temperature-programmed desorption and infra-red investigations of CO adsorption on the various catalysts.

References

1. B. Bailey, M.S. Thesis, University of Utah, Salt Lake City, Utah, 1978.

2. C.H. Yang and A.G. Oblad, ACS Petrol. Div. Preprints, 23 (2), 513 (1978).

Table 1

Adsorption Results on Fe Catalysts

Catalyst	4	44	76
Fe	100	100	100
Mn	0	5	44
Charge wt., mg	328.3	298.5	431.2
Reduced wt., mg	159.1	177.5	140.8
O_2 Adsorption			
mg/g red. cat.	8.7	9.6	7.6
mmol/g red. cat.	0.27	0.30	0.24
mmol/g Fe	0.27	0.32	0.38
CO Adsorption			
mg/g red. cat.	--	6.0	4.2
mmol/g red. cat.	--	0.22	0.15
mmol/g Fe	--	0.23	0.23

Figure 1. Microbalance Results on Fe Catalysts. Numbers on curves refer to catalysts listed in Table 1.

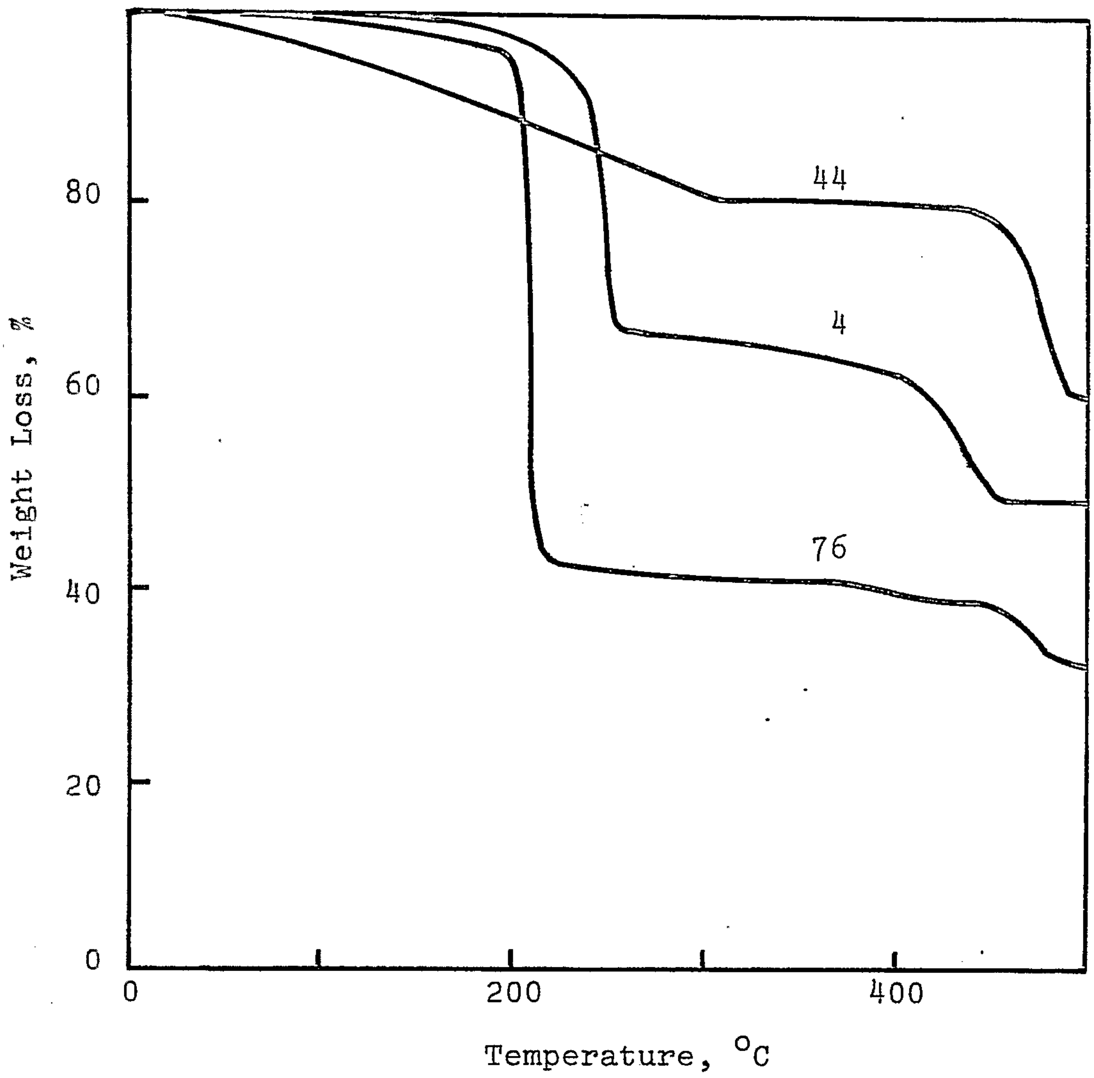

Project A-8

Synthesis of Light Hydrocarbons From CO and H_2

Faculty Advisor: F.V. Hanson
Graduate Student: Y.S. Tsai

Introduction

The hydrogenation of carbon monoxide for the production of low molecular olefins (C_2-C_4) has been investigated over a variety of metallic catalysts. In particular, iron manganese catalysts have exhibited significant selectivity for low molecular weight olefins.

Fourteen Fe/Mn catalysts have been prepared by coprecipitation and tested in a fixed bed reactor. A correlation was made between the product selectivities and catalyst compositions to interpret the catalyst performance. Maximum production of C_2-C_4 hydrocarbons was obtained with a catalyst composed of 2 parts of Mn per 100 parts Fe (atomic ratio), but on the average accounted for only 50% of the total hydrocarbon production. The C_2-C_4 olefins increased with manganese content but dropped sharply above the Mn/Fe ratio of 70. The standard operating conditions were 7-9% CO conversion, 500 psig, 1.06 cc/g/sec space velocity and H_2/CO ratio of 2/1.

Project Status

Fourteen catalysts of different Mn/Fe ratios have been prepared by coprecipitation of iron (III) nitrate and manganese (II) nitrate solution (50%) in ammonium hydroxide. The pH of the solutions were maintained above 9 to insure complete precipitation. The compositions of these catalysts were determined by X-ray fluorescence spectroscopy (Table 1).

The standard catalyst pretreatment consisted of an insitu reduction in flowing hydrogen for 20 hours at 773°K and the ambient pressure. The standard operating conditions for evaluating the catalysts were 500 psig pressure, 1.06 gas hourly space velocity ($cm^3\ g^{-1}s^{-1}$), a hydrogen to carbon monoxide ratio of 2/1 and a temperature range from 485-560°K. The temperature was varied to maintain conversion approximately constant in the range of 5-10%. In addition to the Fe-Mn catalysts tested, pure iron and pure manganese were also tested.

The following preliminary conclusions were drawn from the evaluations of the series of 14 catalysts:

1) The production of C_2-C_4 hydrocarbons was not sensitive to Mn-Fe ratio at standard test conditions.

2) The olefin/paraffin ratio declined significantly for Mn-Fe ratio above ∿75 at standard operating conditions.

3) Methane yield increased above Mn-Fe ratio of 75 at standard operating conditions.

Future Work

The influence of pressure, feed composition and space velocity on a smaller subset of the 14 catalysts prepared for the catalyst composition studies will be determined. A correlation between temperature and conversion for this same subset of catalysts will be developed. The influence in-situ of catalyst pretreatment on selectivity and activity will be determined.

Table 1

Compositions of Fe/Mn Catalysts

Catalyst No.	Atomic Mn/100 Fe Ratio
1	.0
2	1.1
3	2.2
4	3.2
5	4.4
6	5.6
7	8.4
8	11.7
9	17.7
10	41.0
11	63.0
12	109.0
13	278.0
14	607.0

Project B-1

Development of Optimum Catalysts and Supports

Faculty Advisor: F.E. Massoth
Graduate Student: A. Chantong

Introduction

This project involves assessing diffusional resistances within amorphous-type catalysts. Of primary concern is the question of whether the larger, multiringed aromatics found in coal-derived liquids will have adequate accessibility to the active sites of typical processing catalysts. When molecular dimensions approach pore size diameters, the effectiveness of a particular catalyst is reduced owing to significant mass transport resistance. An extreme case occurs when molecular and pore sizes are equivalent, and pores below this size are catalytically inactive.

The project objective can be achieved through a systematic study of the effect of molecular size on sorptive diffusion rates relative to pore geometry. Conceptually, the diffusion of model aromatic compounds is carried out using a stirred batch reactor. The preferential uptake of the aromatic from the aliphatic solvent is measured using a UV spectrometer. Adsorption isotherms are determined to supplement the diffusion studies.

Initial work entailed development of a suitable reactor, measurement techniques and methods of data analysis. These studies, employing chrysene and two different alumina supports, demonstrated that adsorption was diffusion-controlled. Effective diffusivities were larger than predicted for pore diffusion and a surface diffusion contribution was postulated. Subsequent studies were extended to other multiringed aromatic compounds and aluminas with similar results. The fractional surface diffusion contribution was appreciable and about the same in all cases. Because of this, restrictive diffusion effects could not be properly evaluated. However, for the largest size compound (20 Å) and smallest average pore size alumina (50 Å) tested, a markedly lower diffusivity was obtained, indicative of a restrictive diffusion effect.

Project Status

Our major thrust at present is to confirm a restrictive effect on diffusion of large aromatic molecules in small catalyst pores. As discussed in the last report, this requires a knowledge of bulk diffusivities of aromatic-solvent combinations and the catalyst tortuosity factor.[1] In addition an appreciable surface diffusion contribution was found, complicating the analysis for obtaining the restrictive coefficient. The applicable equation is

$$D_e = \left(\frac{D_B \varepsilon}{\tau}\right) K_r + \varepsilon K D_s \qquad (1)$$

where D_e is the overall measured diffusivity, D_B is the bulk diffusivity, D_s is the surface diffusivity, K_r is the restrictive coefficient, K is the equilibrium adsorption constant, ε is the catalyst pore volume, and τ is the tortuosity. Thus, to determine K_r all the others need to be known for the system under investigation.

Bulk diffusivities have not been reported for combinations used in this study. An apparatus for measuring these has been assembled and tested.[1] The exit line from the diffusion coil to the UV cell gave an appreciable dispersion, complicating the analysis for the diffusion coefficient. This has been remedied by shortening this portion of the apparatus, so that the correction for this is now negligible. Tests with a solute-solvent combination reported in the literature showed good agreement within experimental error. For naphthalene in methanol a value of 17.7 (± 1.8) x 10^{-6} cm^2/sec was obtained compared with the literature value of 17.0 x 10^{-6} cm^2/sec at 20°C.[2]

The problem of determining the tortuosity of a given catalyst has been approached by using a small-sized aromatic molecule, such that K_r in Equation (1) can be assumed to be unity. For this purpose naphthalene (6.9 Å) was used with catalyst L (49 Å average pore diameter). Catalyst L was chosen for detailed study because of its expected restrictive effect for larger molecules to be used later. Because of the complication of surface diffusion, the value of D_s not being known, a series of measurements were taken on the same catalyst having different adsorptivities to determine both τ and D_s from the plot of D_e vs. K (Eq (1)).

The adsorptivity of a given catalyst can be changed by subjecting the catalyst to different calcination temperatures.[3] The catalyst is first calcined at 500°C to fix its structure. It is then exposed to laboratory air, from which it rapidly picks up water. This water adsorbs on acidic sites rendering them inactive for the adsorption of aromatics.[4] When subjected to a subsequent calcination, the catalyst loses some of this water, reactivating some adsorption sites, the amount depending upon the calcination temperature employed. The structural properties of the catalyst will not change, e.g., pore volume, average pore diameter, since these have been set by the original calcination.

This procedure was adopted for measurements of naphthalene (in cyclohexane) diffusivity in catalyst L. By varying the calcination temperature between 65° and 500°C, values of K from 14 to 90 were obtained. Figure 1 shows the variation of measured diffusivity as a function of K for this system at room temperature. Earlier data[3] agree quite well with the new data. Least squares analysis of the straight line gave $\tau = 1.7 \pm 0.2$, which is not an unreasonable value for alumina catalysts.[5]

Since to a first approximation the tortuosity is a property of the catalyst only, it should not change appreciably with the solute-solvent combination used. Therefore this value should be valid for studying diffusion of larger molecules, and hopefully K_r then can be calculated for the latter cases by use of Equation (1).

Future Work

Bulk diffusivity measurements will be made on another known combination to check the accuracy of the method before going on to the unknown systems. Diffusion measurements of larger aromatics in catalyst L will be undertaken.

References

1. W. H. Wiser *et al.*, DOE Contract No. E(49-18) - 2006, Quarterly Progress Report, Salt Lake City, Utah, July-Sept 1978.

2. International Critical Tables, Vol 5, p 73.

3. W.H. Wiser *et al.*, DOE Contract No. E(49-18) - 2006, Quarterly Progress Report, Salt Lake City, Utah, July-Sept 1977.

4. M. Moora, M.S. Thesis, University of Utah, Salt Lake City, Utah, 1977.

5. C. Satterfield, "Mass Transfer in Heterogeneous Catalysis," MIT Press, Cambridge, Massachusetts, 1970.

Figure 1. Diffusivity vs. Adsorption.

Catalyst L

Naphthalene in Cyclohexane

○ Current Data

□ Data of Reference 3

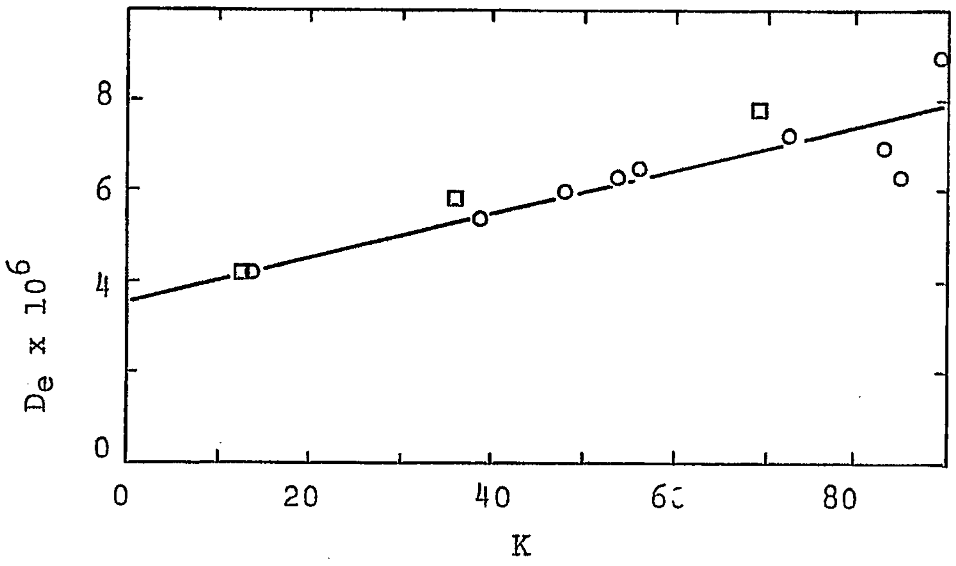

Project B-2 (alternate)

The Effects of Poisoning on the Desulfurization Activity of Cobalt-Molybdate Catalysts

Faculty Advisor: F.E. Massoth
Graduate Student: R. Ramachandran

Introduction

The importance of cobalt-molybdena catalysts for hydrotreating and hydrodesulfurization of petroleum feed stocks is well known. These catalysts are also being studied for hydrodesulfurization and liquefaction of coal slurries and coal-derived liquids. However, these complex feed stocks result in rapid deactivation of the catalysts. To gain an insight into the deactivation mechanism, detailed kinetics of the hydrodesulfurization of the model compound benzothiophene are compared before and after addition of various poisons and coke precursors. The studies are planned using a constant stirred microbalance reactor, which enables simultaneous measurement of catalyst weight change and activity.

Initial tests with the flow microbalance reactor showed that perfect gas mixing was not achieved when injecting a liquid feed (gaseous at reaction temperature) directly into the reactor. Modifications were incorporated into a new reactor design which have eliminated the problem and improved the mechanical stability of the system.

Preliminary tests of the benzothiophene hydrodesulfurization reaction showed the rate to be proportional to benzothiophene and hydrogen and inhibited by benzothiophene and H_2S. Pyridine and quinoline were poisons for the reaction. Advantage of this finding was taken to develop a technique for assaying active catalyst sites by successive poisoning-activity measurements.

Adsorption of H_2S on the sulfided catalyst was reversible and could be correlated with the Langmuir adsorption isotherm. Chemisorption of pyridine lowered H_2S adsorption, indicating a competition for adsorption sites. Temperature programmed desorption studies of thiophene also showed quinoline to compete with thiophene for adsorption sites.

Project Status

Temperature programmed desorption studies were continued using hydrogen sulfide. Preliminary results indicated the following: (1) γ-alumina showed two distinctive types of adsorption sites with activation energies of desorption of 15 and 30 kcal/mole. (2)The presence of quinoline decreased the amount of H_2S adsorbed and decreased both activation energies. (3) For the CoMo catalyst, the temperature range of the first peak corresponded to that of alumina whereas the second peak shifted to a higher temperature. The second peak may be due to active sites on MoS_2 based on experiments using MoS_2. (4) The presence of quinoline reduced the H_2S adsorption of the CoMo catalyst.

Future Work

Detailed analysis of the temperature programmed desorption studies and further experiments to substantiate the results will be carried out. Preliminary experiments to establish the satisfactory range of reactor performance will be run before proceeding to the kinetic runs using benzothiophene.

Project B-4

Mechanism of Catalytic Hydrogenation by Metal Halide Catalysts

The Initial Stage of Coal Hydrogenation in the Presence of Catalysts

Faculty Advisor: D.M. Bodily
Postdoctoral Fellow: R. Yoshida

Introduction

Studies of the treatment of coal with hydrogen under mild reaction conditions indicate that the benzene-soluble products from the initial stages of the reaction are structurally different from the products obtained at longer reaction times. These products may originate from structurally different portions of the original coal. Kinetic studies of coal hydrogenation show that the reaction may be divided into two stages, an initial stage where the rate of reaction is rapid and a second stage where the reaction rate is comparatively slower.

The reaction rate of the initial stage is related to coal parameters such as volatile matter and fixed carbon content. These parameters are related to the thermal reactions which occur upon heating. The soluble products of the first stage are of relatively low molecular weight and could be attributed to the thermal reactions occurring in the initial stages of the reaction. The reaction rate of the second step is independent of coal rank. These results could also be interpreted in terms of a dual structural system in coal.

Hydrogasification of coal also occurs in two stages. The initial stage is very rapid while the second stage is much slower. Rate constants for the initial stage are proportional to the volatile matter of the feed coal, but at higher conversions the rate constants for all coals approach one another. Optimum conditions for the formation of organic liquid products during the initial stage have been determined.

Pyrolysis and dissolution of a high-volatile Utah coal have been discussed and compared with hydrogenation. These reactions involve an initial rapid process followed by a slower process. The original coal may contain considerable quantities of nonaromatic and low molecular weight aromatic constituents which can be liberated through purely thermal rupture and internal stabilization of bonds during the initial stage. A recent study on flash heating of high volatile coal indicates that coal is composed of at least two very different structures, and the result of flash heating is the evolution of smaller molecules less tightly bound. The yield of these molecules is proportional to volatile matter content.

The postulate of a dual structure in coal is consistent with results of mass spectrometry and solvent extraction experiments on coal.

When coal hydrogenation is considered in terms of a dual structure model, the initial stage of the reaction is of great importance in the design of a hydrogenation process. The initial stages of coal hydrogenation will be studied using several catalyst systems.

Project Status

Clear Creek, Utah coal (0.83% H_2O, 6.50% ash, 45.42% VM and 47.25% FC) was hydrogenated in a short-residence, coiled-tube reactor. Zinc chloride, Co-Mo/Al_2O_3, red-mud plus sulfer and presulfided red-mud were used as catalysts. The particle size was -100, +200 mesh and the catalyst ranged from 6.4% for $ZnCl_2$ to 10.7% for the others. Coal was also hydrogenated without catalyst. The temperature ranged from 400°C to 500°C and the hydrogen pressure was 1800 psi. Residence time (8 - 372 sec) was varied by choice of the tube length (40 - 120 ft).

Products were separated by stepwise extraction using hexane, toluene and pyridine. Determination of C,H and N for each product was carried out by a micro method using a Perkin-Elmer 240 Elemental Analyzer. Proton NMR spectra were measured at 90 MHz and 300 MHz. The results of ultimate analysis of each product are shown in Tables 1-4 and Figures 1 and 2. The H/C atomic ratio decreases with increasing conversion, especially up to 20% conversion. The changes in liquid (oil + asphaltene-I) and asphaltene-II are also remarkable. The O,N,S/C atomic ratio increases with conversion up to 20%, and it is nearly constant in spite of the progress of conversion beyond 20%. At about 20% conversion the H/C ratio of each product for $ZnCl_2$ catalyst is lower than for other catalysts. This suggests that $ZnCl_2$ catalyzes reactions which decrease the H/C ratio.

Typical proton NMR spectra of liquid (oil + asphaltene-I) measured at 90 Hz and 300 MHz are compared in Figure 3. In the 300 MHz spectra two new bands can be discerned in the aliphatic region at 1.5 $\sim$ 1.8 ppm[1] and 2.0 $\sim$ 2.1 ppm. The hydrogen distribution of each product obtained from NMR spectra is shown in Tables 1-3. Hydrogens bound to aromatic carbons, H_a, and hydrogens bound to carbons α to aromatic rings, H_α, increase. The hydrogens bound to aliphatic carbons β or further from aromatic rings, H_o, decrease with increasing conversion.

Structural analysis was performed using the equation of Brown and Ladner.[2,3] Results of these calculations are shown in Tables 1-3 and Figure 4. The carbon aromaticity , f_a, increases and the aromatic hydrogen to carbon ratio of the hypothetical unsubstituted aromatic material, H_{au}/C_a, decreases with the increase of conversion. Up to 20% conversion the changes in liquid (oil + asphaltene-I) and asphaltene-II are significant. The main differences in the chemical structure between liquid (oil + asphaltene-I) and asphaltene-II are the average number of aromatic rings in the unit structure (H_{au}/C_a) and f_a. At about 20% conversion the degree of substitution of ring carbons, σ, of each product using $ZnCl_2$ catalyst is lower, and f_a is higher than those obtained with the other catalysts. This suggests that $ZnCl_2$ catalyzes reactions which decrease σ and increase f_a, e.g., dealkylation. This ability of $ZnCl_2$ may be related to the high activity in the initial stage of hydrogenation.

A continuous distribution may exist in the structural units of coal. The units taking part in the noncatalytic reaction up to about 20% conversion are characterized by a higher H/C ratio, lower O, N, S/C ratio, higher content of aliphatic hydrogen (H_α + H_o), lower f_a and 1-2 aromatic rings. In the catalytic reaction (greater than 20% conversion) the units taking part are characterized by lower H/C raio, higher content of H_a, higher f_a and larger number of aromatic rings.

Future Work

Toluene-insolubles will be further extracted with pyridine. Structural analysis of pyridine-solubles will be performed. An average molecular unit of the various products will be considered in terms of structural parameters calculated by the equation of Brown and Ladner and molecular weights measured by vapor pressure osmometry.

References

1. K.D. Bartle and D.W. Jones, Fuel, 48, 21 (1969)

2. J.K. Brown and W.R. Ladner, Fuel, 39, 87 (1960)

3. G. Takeya, M. Itoh, A. Suzuki and S. Yokoyama, Nenryo Kyokaishi (J. Fuel Soc. Japan), 43, 837 (1964).

Table 1. Ultimate Analysis, Atomic Ratio, Hydrogen Distribution and Structural Parameters of Liquid (Oil + Asphaltene - I).

Catalyst	Temp	Time	Ultimate Analysis (%, DAF)				Atomic Ratio		Hydrogen Distribution			Structural Parameters*			
	(°C)	(sec)	C	H	N	O+S(diff)	H/C	O,N,S/C	H_a	H_α	H_o	f_a	σ	$\frac{H_{au}}{C_a}$	$\frac{H_o}{H_\alpha}$
$ZnCl_2$	400	13	84.9	9.6	0.3	5.2	1.36	0.05	0.157	0.223	0.620	0.43	0.48	0.97	2.8
	450	13	84.2	8.9	0.6	6.3	1.27	0.07	0.176	0.206	0.618	0.48	0.45	0.87	3.0
	500	8	--	--	--	--	--	--	--	--	--	--	--	--	--
		21	81.9	8.8	0.8	8.5	1.29	0.09	0.176	0.227	0.598	0.47	0.50	0.97	2.6
		372	85.4	8.2	1.4	5.0	1.15	0.06	0.239	0.263	0.497	0.57	0.43	0.84	1.9
Co-Mo	500	12	83.9	9.9	0.6	5.6	1.41	0.06	0.171	0.204	0.625	0.42	0.45	1.03	3.1
Pre-Sulfided Red-Mud	500	12	84.2	9.8	0.6	5.4	1.40	0.05	0.109	0.221	0.670	0.38	0.58	0.96	3.0
Red-Mud Plus Sulfur	500	12	83.8	9.7	0.6	5.9	1.39	0.06	0.110	0.178	0.712	0.38	0.54	0.89	4.0
No		10	81.0	8.0	1.1	9.9	1.19	1.10	0.175	0.289	0.536	0.51	0.56	0.95	1.9

---

*f_a - Carbon aromaticity.

σ - The degree of substitution of ring carbons.

H_{au}/C_a - The atomic aromatic hydrogen-to-carbon ratio of the hypothetical unsubstituted aromatic material.

H_o/H_α - A measure of the length of the aliphatic carbon chain.

Table 2. Ultimate Analysis, Atomic Ratio, Hydrogen Distribution and Structural Parameters of Asphaltene-II.

Catalyst	Temp (^{o}C)	Time (sec)	Ultimate Analysis (%,DAF)				Atomic Ratio		Hydrogen Distribution			Structural Parameters			
			C	H	N	O + S	H/C	O,N,S/C	H_a	H_α	H_o	f_a	σ	$\frac{H_{au}}{C_a}$	$\frac{H_o}{H_\alpha}$
$ZnCl_2$	400	13	86.4	9.7	1.1	2.8	1.35	0.03	0.123	0.180	0.697	0.40	0.50	0.80	3.9
	450	13	85.6	8.6	0.6	5.2	1.21	0.05	0.160	0.243	0.596	0.49	0.50	0.78	2.5
	500	8	84.8	8.1	0.7	6.4	1.15	0.06	0.199	0.248	0.553	0.54	0.44	0.77	2.2
		21	85.2	7.6	0.8	6.4	1.07	0.06	0.220	0.315	0.465	0.58	0.50	0.81	1.5
		372	86.6	6.8	0.9	5.7	0.94	0.06	0.231	0.252	0.517	0.63	0.45	0.63	2.1
Co-Mo	500	12	84.8	8.8	0.7	5.7	1.25	0.06	0.127	0.231	0.641	0.45	0.57	0.83	2.8
Pre-Sulfided Red-Mud	500	12	83.9	8.4	0.9	6.8	1.20	0.07	0.155	0.185	0.659	0.49	0.48	0.76	3.6
Red-Mud Plus Sulfur	500	12	84.3	8.8	0.9	6.0	1.25	0.06	0.133	0.200	0.667	0.46	0.54	0.76	3.3
No		10	84.4	8.5	0.7	6.4	1.21	0.06	0.138	0.245	0.617	0.48	0.55	0.78	2.5

Table 3. Ultimate Analysis, Atomic Ratio, Hydrogen Distribution and Structural Parameters of Oil.

Catalyst	Temp	Time	Ultimate Analysis (%,DAF)				Atomic Ratio		Hydrogen Distribution			Structural Parameters			
	(^{o}C)	Sec	C	H	N	O+S(diff)	H/C	O,N,S/C	H_a	H_α	H_o	f_a	σ	$\frac{H_{au}}{C_a}$	$\frac{H_o}{H_\alpha}$
$ZnCl_2$	400	13	85.6	9.6	0.5	4.3	1.35	0.04							
	450	13	85.7	10.1	0.2	4.0	1.41	0.04	0.128	0.252	0.620	0.38	0.57	1.11	2.5
	500	8	84.5	9.9	0.2	5.4	1.41	0.05							
		21	84.3	9.6	0.4	5.7	1.37	0.05							
		372	85.9	8.2	1.4	4.5	1.15	0.05	0.216	0.294	0.490	0.54	0.46	0.87	1.7
Co-Mo	500	12	84.4	10.3	0.1	5.3	1.46	0.05							
Pre-Sulfided Red-Mud	500	12	84.4	10.3	0.3	5.0	1.46	0.05							
Red-Mud Plus Sulfur	500	12	84.9	10.5	0.0	4.6	1.48	0.04							
No		10	84.5	10.3	0.0	5.2	1.46	0.05							

Table 4

Ultimate Analysis and Atomic Ratio of Asphaltene - I

Catalyst	Temp (°C)	Time (sec)	Ultimate Analysis (%, DAF) C	H	N	O + S	Atomic Ratio H/C	O,N,S/C
$ZnCl_2$	400	13	80.8	7.6	1.2	10.4	1.13	0.11
	450	13	79.4	7.5	1.5	11.6	1.13	0.12
	500	8	78.5	7.2	1.7	12.6	1.10	0.14
		21	79.3	7.4	1.4	11.9	1.12	0.13
		372	80.9	6.3	1.2	11.6	0.93	0.12
Co-Mo	500	12	78.0	7.6	1.6	12.8	1.16	0.14
Pre-Sulfided Red-Mud	500	12	79.6	7.4	1.5	11.5	1.12	0.12
Red-Mud Plus Sulfur	500	12	78.6	7.7	0.8	12.9	1.18	0.13
No		10	81.9	7.5	1.1	9.5	1.10	0.10

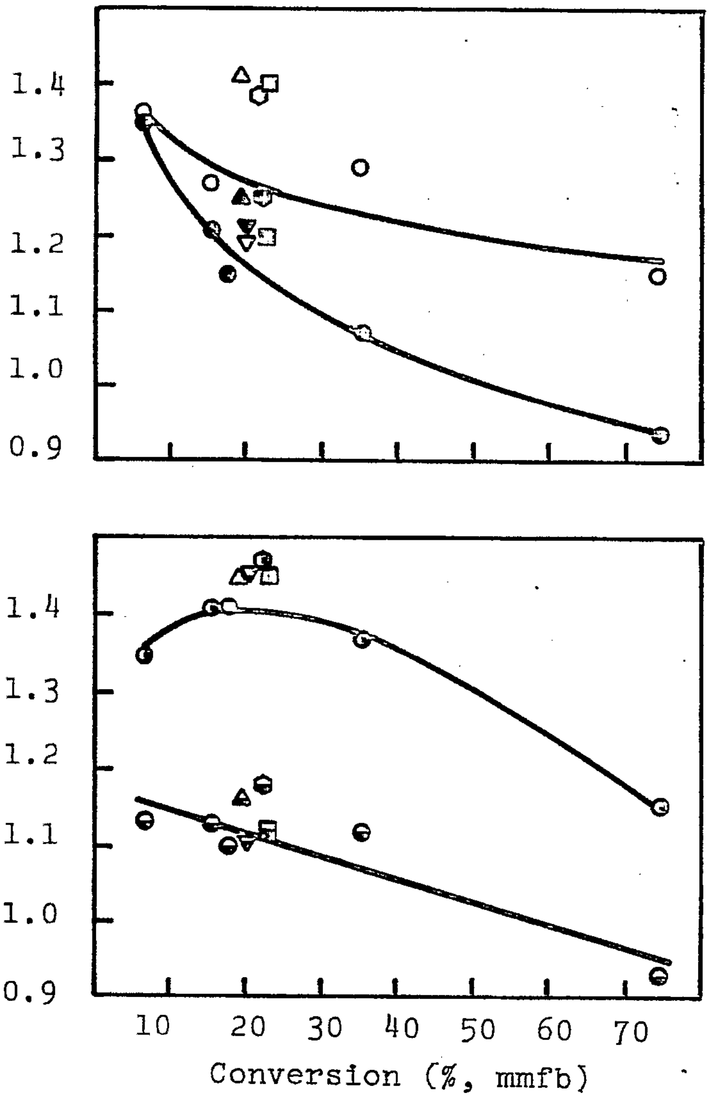

Figure 1. Change of atomic ratio H/C of products with conversion.

	Liquid	Asphaltene-II	Oil	Asphaltene-I
$ZnCl_2$	○	◐	⊙	⊖
Co-Mo	△	▲	◬	◬
Presulfided Red-Mud	□	◧	⊡	⊟
Red-Mud plus Sulfur	⬡	⬢	⬡	⬡
No Catalyst	▽	▼	▽	▼

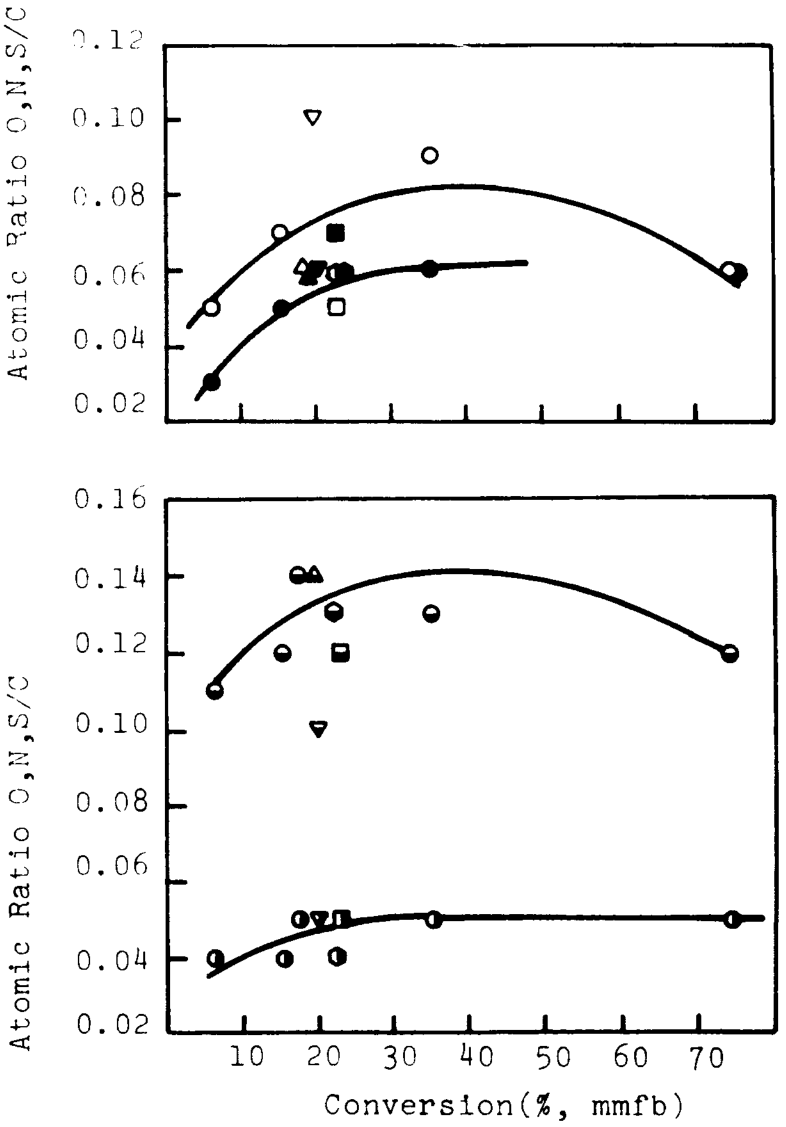

Figure 2. Change of atomic ratio O, N, S/C of products with conversion.

	Liquid	Asphaltene-II	Oil	Asphaltene-I
$ZnCl_2$	○	●	◐	⊖
CO-Mo	△	▲	▲	▲
Presulfided Red-Mud	□	■	◧	⬒
Red-Mud plus Sulfur	⬡	⬢	⬢	⬢
No Catalyst	▽	▼	▼	▼

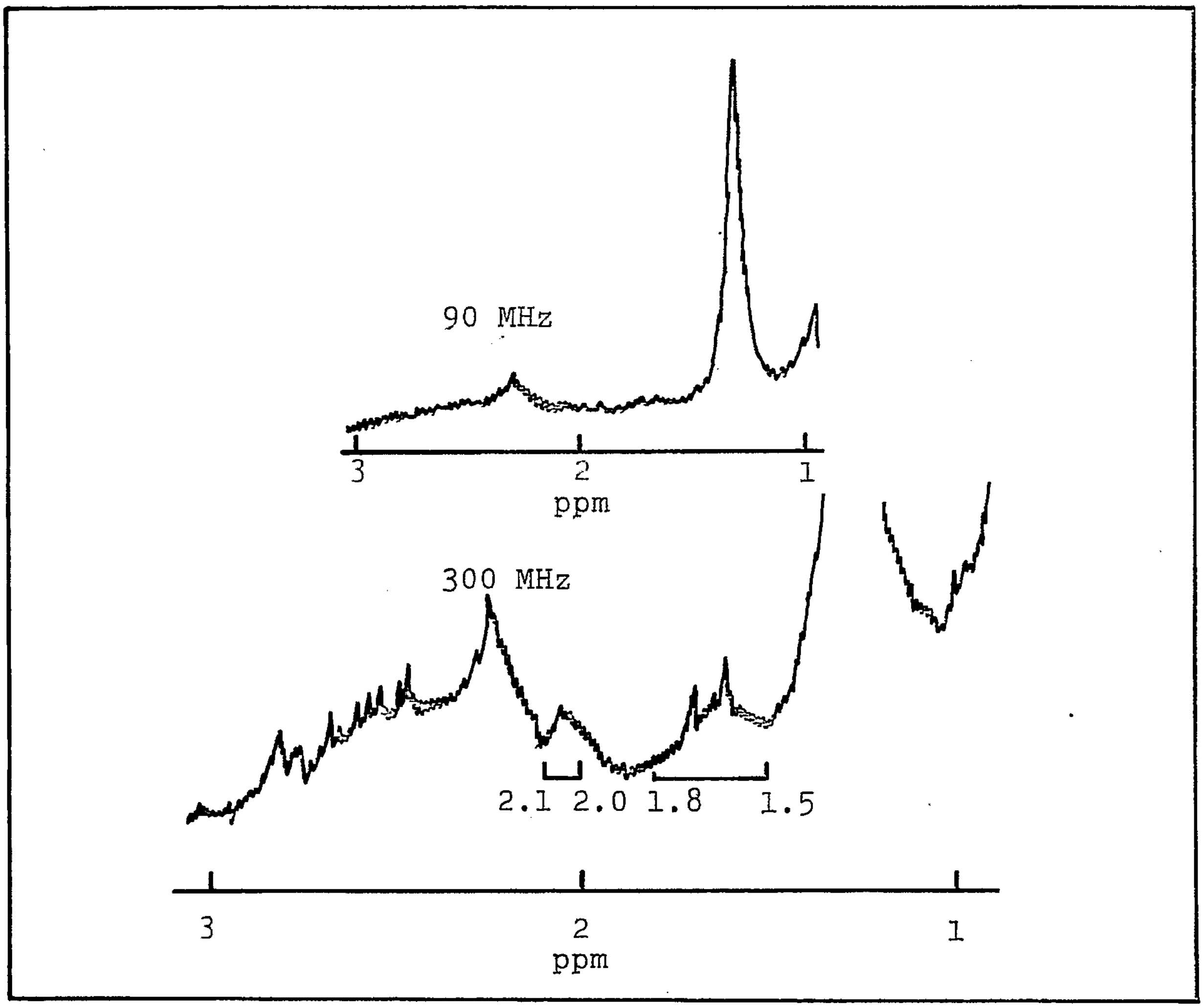

Figure 3. Aliphatic region of proton NMR spectra of liquid (oil + asphaltene-I) measured at 90 MHz and 300 MHz.

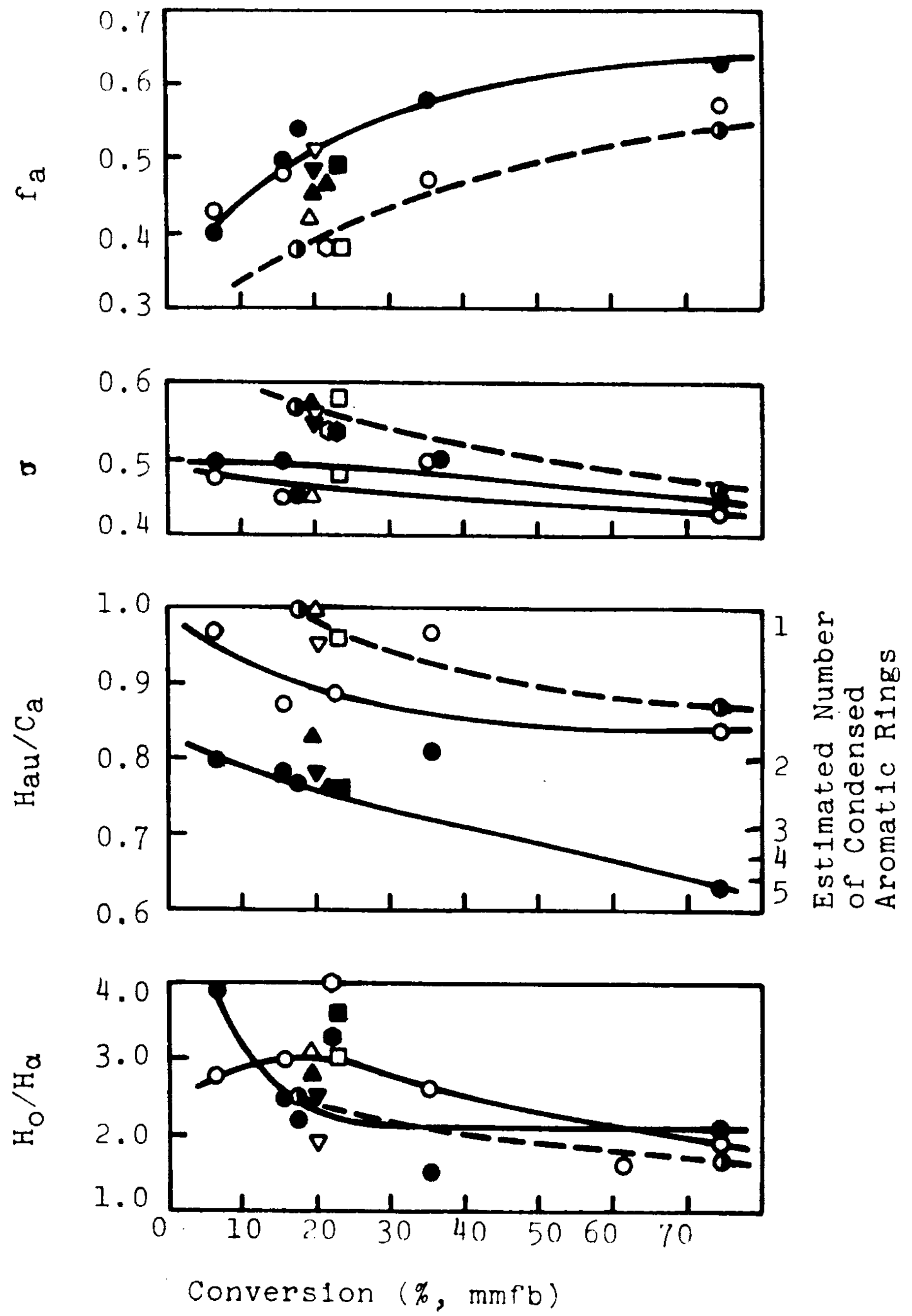

Figure 4. Change of structural parameters of products with conversion.

	Liquid	Asphaltene-II	Oil
$ZnCl_2$	○	●	◐
Co-Mo	△	▲	
Presulfided Red-Mud	□	■	
Red-Mud plus Sulfur	⬡	⬢	
No Catalyst	▽	▼	

Project B-4

Mechanism of Catalytic Hydrogenation by Metal Halide Catalysts

IR Studies of Coal Metal Salts Interactions

Faculty Advisor: R.E. Wood
Graduate Student: Doug Stuart

Introduction

Coal catalyst interactions are being investigated using Infrared Spectroscopy. Various coal structures have been associated with peaks in the IR spectrum. These peaks are being compared for different coals and chars to monitor changes in the associated structure.

Sample particle size and potassium bromide-water contamination were identified last quarter as two important parameters to be controlled in sample preparation. Possible procedures were also mentioned.

Project Status

To determine the relative importance of the parameters, five similar samples were prepared and each was ground for a different length of time. The results are shown in Figure 1. Scatter was measured as log (% transmittance at 1850 cm^{-1}/ % transmittance at 3800 cm^{-1}), potassium bromide-water contamination was calculated as the absorbance at 3440 cm^{-1} divided by the sample weight, and the sample absorptivity was calculated as the absorbance at 2920 cm^{-1} divided by the sample weight. A sample must be ground at least 10 minutes to obtain a constant sample absorptivity and at least 20 minutes to achieve a constant background scatter (Figure 1). In both cases the potassium bromide-water contamination is large.

It is possible to avoid much of the $KBr-H_2O$ contamination by grinding for a shorter period and using less KBr. Three similar samples of the same coal were prepared by first grinding 10 mg of coal with 90 mg KBr, weighing 10 mg of this mixture and adding 490 mg of KBr, then grinding for five more minutes. The background scatter was equivalent to grinding 30 minutes. The $KBr-H_2O$ peaks were reduced, but were not as reproducible as other peaks in the spectrum (16% compared with 3%). The procedure also involved twice as much sample handling.

Heating the sample pellets for several hours at temperature between 110°C and 150°C significantly reduced the $KBr-H_2O$ peaks at 3440 cm^{-1}, 2000 cm^{-1} and 1610 cm^{-1} without otherwise affecting the spectrum except for a small peak that grew at 2340 cm^{-1} depending on the amount of heating. Three samples of one coal were prepared using the dual grind procedure described above. Each were compared before heating, after 20 hours at 130°C and 18 inches vacuum and after 60 hours at 130°C and 18 inches vacuum. The KBr-H_2O contamination, which before heating varied considerably, became uniform for the three samples after 20 hours and remained constant after 60 hours heating.

The use of a new pellet die allowed the samples to be heated and still obtain a uniform KBr-H_2O contamination. The following sample preparation procedure has an expected reproducibility of less than 3% error.

1. Weigh 1 mg sample and record weight.
2. Add KBr to a total weight of 450 mg and record weight. (KBr previously dried overnight at 130°C.)
3. Grind sample 25 minutes.
4. Weigh 400 mg for a pellet and record weight.
5. Place the sample in a heated die, evacuate and press at 7 tons for 10 minutes.
6. Remove pellet from the die and place in the vacuum dessicator overnight (130°C at 18 inches vacuum).
7. Record spectra under nitrogen avoiding air contact as much as possible.
8. Measure thickness of the pellet.

Future Work

There have been problems in pressing a uniformly clear pellet. Work will be aimed at obtaining such a pellet before the reproducibility of the procedure is determined. A check will be made to be sure the sample concentrations are in the linear Beer's law range and the sample and char spectra will be run.

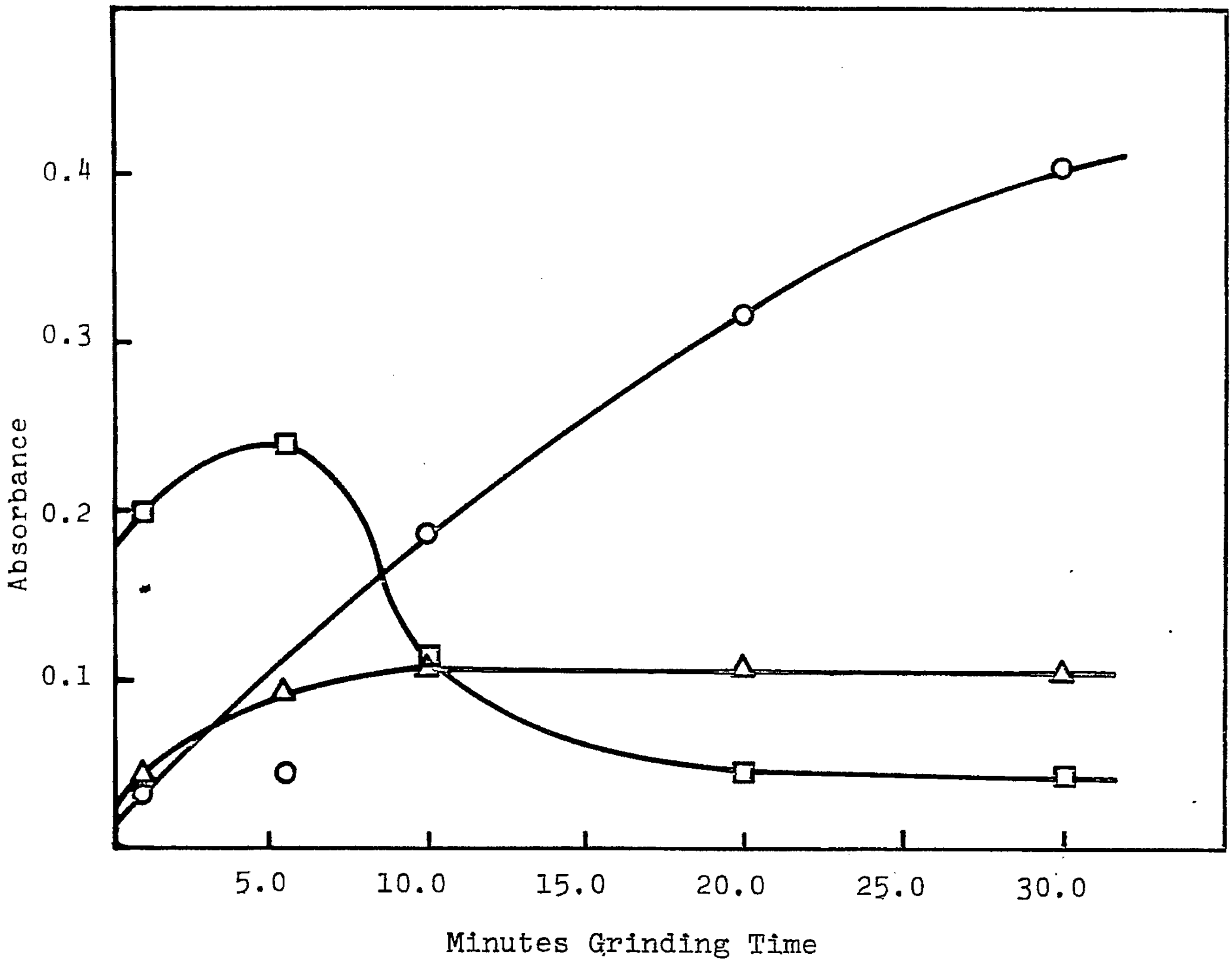

Figure 1. The effects of grinding time on the IR spectrum of coal. Scatter □; Potassium bromide-water contamination ○; Sample absorptivity △.

Project C-2

Heat Transfer to Gas-Solid Suspensions in Vertical Cocurrent Downflow

Faculty Advisor: J.D. Seader
Graduate Students: J.M. Kim
B. Scott Brewster

Introduction

This project is concerned with an investigation of the mechanisms of heat and momentum transport for gas-solid suspensions flowing vertically downward through heated tubes. The results have applicability in the design of short-residence time, continuous, coal-hydrogenation reactors. Motivation for conducting this research is provided by the lack of data or correlations in the literature pertaining specifically to the cocurrent downflow configuration. Experiments are being conducted with glass bead-air and coal particle-air systems.

Project Status

To find a guide for correlating the pressure drop and heat transfer data for the glass bead-air system, a similarity analysis was made on the suspension conservation equations. Hellums and Churchill present a procedure for finding the minimum number of dimensionless groups in the governing differential equations.[1] Their method, when applied to the steady-state fully developed flow condition, yields the following equation for the parametric description of the pressure drop:

$$\frac{\Delta P_f}{\frac{1}{2}\rho_g U_{gi}^{\,2}} = \phi\left[\frac{1}{N_{Re,sg}}, \frac{\rho_{dp}}{\rho_{dg}}, \frac{W_p}{W_g}, \frac{\mu_{pm}}{\mu_{gm}}, \frac{C_D E_{pi} D}{d_p(1-E_{pi})} N_{Re,sg}, \frac{gD}{U_{gi}^{\,2}} N_{Re,sg}\right] \quad (1$$

For dilute-suspension flow the term $\frac{\mu_{pm}}{\mu_{gm}}$ is of minor importance.

The relative importance of the other parameters is not fully understood yet. Future study of the experimental data will clarify the effect of each term more clearly.

A comparison of Equation (1) with Rose and Duckworth's correlation[2], which was derived by the Rayleigh index method (Equation 2), shows several interesting points. Their correlation is:

$$\frac{f_p}{f_o} = \phi_1\,(N_{Re,sg})\ \phi_2\frac{(d_p)}{D}\ \phi_3\ \frac{(W_p)}{W_g}\ \phi_4\ \frac{(U_{gi}{}^2)}{gD}\ \phi_5\ \frac{(\rho_p)}{\rho_g} \qquad (2)$$

where $f_p = \frac{\tau_{wp}}{\frac{1}{2}\rho_p U^2{}_{sg}}$

In Equation (2), ρ_p/ρ_g and d_p/D are treated as separate parameters, whereas in Equation (1) only the dispersed density ratio, ρ_{dp}/ρ_{dg}, appears as a parameter and d_p/D effect is combined into the term $\frac{C_D E_{pi} D}{d_p(1-E_{pi})} N_{Re,sg}$ which represents the drag force effect between the gas and particles.

In addition to the similarity analysis, models based on the macroscopic force balance and the single particle motion equation, modified to include the particle concentration effect and the frictional resistance with the wall, are also being studied. Mathematical descriptions of these models will be presented in the next report.

The governing equations for gas and particle temperature for gas-solids flow through a duct where heat transfer is taking place are dependent upon the gas-to-particle heat transfer coefficient. If the solids and gas are in thermal equilibrium at all times (infinite heat transfer rate between gas and particles), the governing equation becomes

$$\frac{dT}{dx} = \frac{D\pi(q/A)_x}{W_g c_g + W_s c_s} \qquad (3)$$

where radiation between the wall and particles and internal particle temperature gradients have been neglected. This equation can be solved with the appropriate boundary conditions to obtain the following expression for local Nusselt number:

$$Nu_x = \frac{h_x D}{k_g} = \frac{\frac{D}{k_g}\ (q/A)_x}{T_W - \left[T_o + \frac{\int_o^x \pi D(q/A)_x dx}{W_g c_g + W_s c_s}\right]} \qquad (4)$$

However, if the gas-to-solids heat transfer rate is finite, the governing equations become

$$\frac{dT_p}{dx} = A\ (T_g - T_p) \tag{5}$$

$$\frac{dT_g}{dx} = B - C\ (T_g - T_p) \tag{6}$$

and analytical solution yields

$$T_p(x) = T_o - \frac{AB}{(A+C)^2}(1-e^{-(A+C)x}) + \frac{AB}{A+C}\ x \tag{7}$$

$$T_g(x) = T_o + \frac{BC}{(A+C)^2}(1-e^{-(A+C)x}) + \frac{AB}{A+C}\ x \tag{8}$$

where

$$A = \frac{A_p}{V_p} \cdot \frac{\frac{k_g}{D}\ Nu_p}{\rho_s u_p c_s}, \quad B = \frac{D\pi\,(q/A)_x}{W_g c_g}, \quad C = A \cdot \frac{W_s c_s}{W_g c_g} \tag{9}$$

Thus knowledge of both the particle velocity and Nusselt number is required for evaluation of the gas or particle temperature at any axial location. Once the local gas temperature has been evaluated, the local wall-to-gas Nusselt number can be calculated from the measured local wall temperature.

$$Nu_x = \frac{h_x D}{k_g} = \frac{(q/A)_x D}{k_g (T_w - T_g)} \tag{10}$$

The local value of the Nusselt number was evaluated for various values of particle velocity and particle Nusselt number from data obtained for the downflow of glass bead-air suspensions (Kim Run No. WSG-83). The results are shown graphically in Figure 1. The local Nusselt number is a rather weak function of particle velocity, but is nevertheless quite important. The Nusselt number for gas alone (Spalding equation) is also shown for comparison. Since the local value of the Nusselt number almost always decreases with distance from the tube entrance and approaches an asymptotic value, the asymptotic value of the Nusselt number with solids present must be less than the asymptotic value of gas alone at the same mass flow rate. However, the exact value cannot be determined without measuring the gas or solids temperature directly.

The present method of determining solids flow rate is unsatisfactory for obtaining pressure drop data for the cocurrent downflow of coal-air suspensions. The method requires sampling of the stream for a short length of time and then weighing of the sample. Since several measurements must be made to obtain an average value, the process becomes quite time consuming. The method also requires direct, open handling of the coal particles with an accompanying dust problem.

To avoid direct contact with the coal and to obtain the best average value of solids flow rate possible for a given run, the weight of the entire amount of solids that flow during a given run will be used to determine the flow rate. Accordingly, the lower (receiving) hopper has been relocated on a platform scale and all of the hopper connections are flexible so that the weight of the hopper contents may be determined before and after the run. With the new method, it will be necessary to ensure that the run is long enough to minimize the transient effects associated with feeder startup and that the pressure drop and, hence, feed rate remain constant throughout the run.

Additional modifications of the experimental equipment include mounting the vibratory feeder and hopper on a special frame, which will keep them in fixed relative position and prevent physical contact between the vibrating trough and hopper downspout. The solid state feedback control for the feeder is not functioning properly and a new controller without the feedback circuitry has been ordered.

Future Work

During the next quarter, design correlations for the pressure drop and the heat transfer coefficient for the glass bead-air system will be obtained by testing the proposed models with the experimental data obtained in this research. Also the equipment modifications to the coal particle-air system will be completed and the pressure drop and particle velocity data taken. The heat transfer section will then be fabricated and tested.

References

1. J.D. Hellums and S.W. Churchill, AIChE J. 10, 110 (1964).

2. H.E. Rose and R.A. Duckworth, The Engineer, 227 (5903), 392 (1969).

Nomenclature

Roman Letters:

A, B, C	Constants
A_p	Particle surface area, ft^2
C_D	Drag coefficient
D	Tube inside diameter, ft
E_{pi}	Particle fraction factor
$N_{Re,sg}$	Reynolds number based on superficial gas velocity
Nu	Nusselt number
T	Temperature, ^oF
T_o	Inlet temperature, ^oF
U_{gi}	Inlet gas velocity, ft/sec
V	Volume, ft^3
W	Mass flow rate, lbm/hr
W_p, W_g	Particle and gas mass flow rate, lbm/hr
c	Heat capacity, Btu/lbm
d	Particle diameter, ft
d_p	Particle diameter, ft
f	Friction factor for gas alone
f_p	Particle friction factor
g	Gravitational constant, ft/sec^2
h_x	Local heat transfer coefficient
k	Thermal conductivity
$(q/A)_x$	Local wall heat flux
u	Velocity
x	Distance from inlet of heated section

Greek Letters:

$\Delta\rho_f$	Frictional pressure drop
ρ	Density
ρ_{dp}, ρ_{dg}	Dispersed particle and gas density, lbm/ft^3
ρ_p, ρ_g	Particle and gas density, lbm/ft^3
τ_{wp}	Particle-wall shear stress, lbf/ft^2

Subscripts:

g	Gas
p	Particle
s	Solids
w	Wall

Figure 1. Dependence of Local Nusselt No. on Particle Velocity and Particle Nusselt No. (Kim Run No. WGS-83).

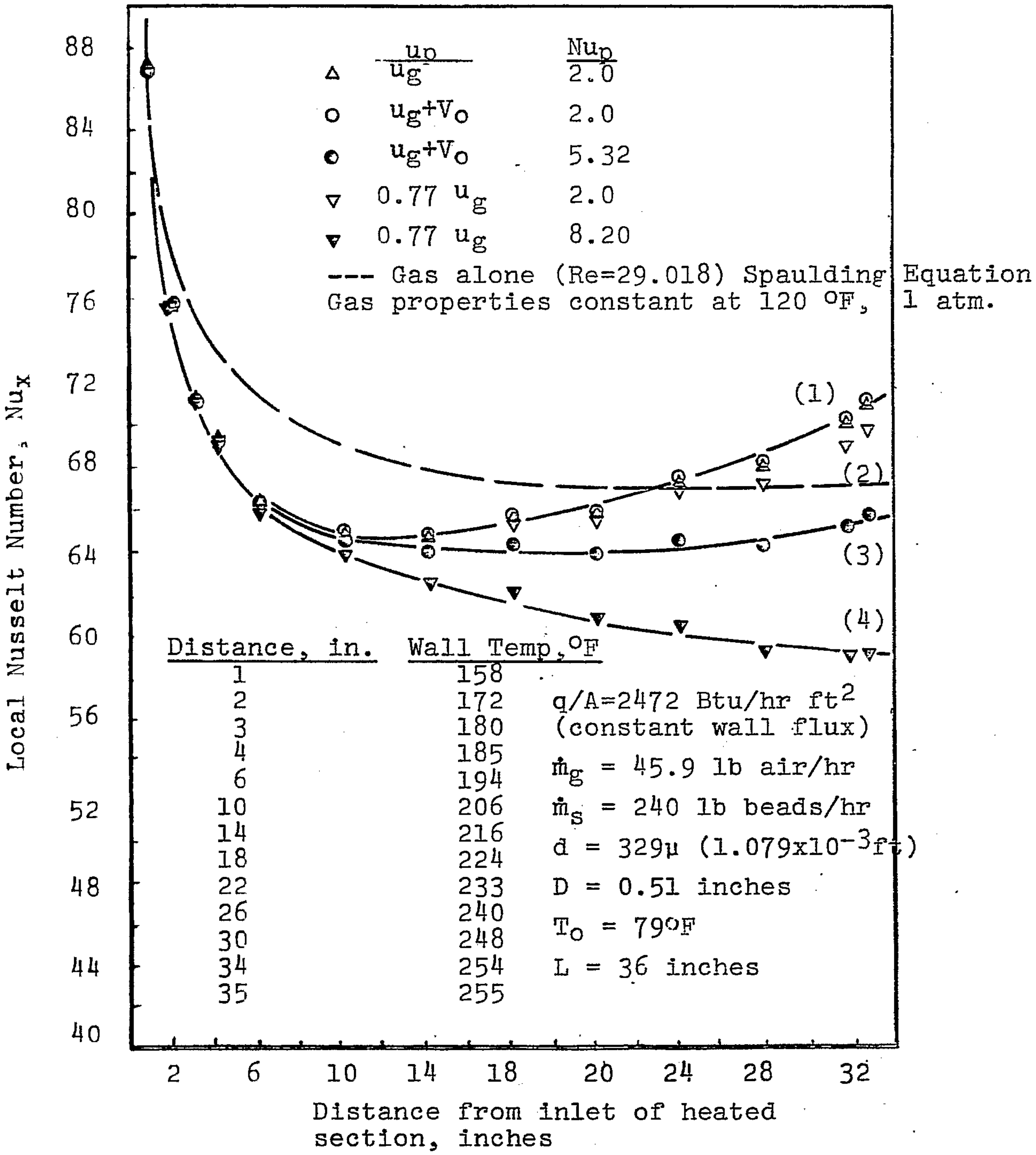

Distance, in.	Wall Temp, °F
1	158
2	172
3	180
4	185
6	194
10	206
14	216
18	224
22	233
26	240
30	248
34	254
35	255

q/A=2472 Btu/hr ft^2
(constant wall flux)
$\dot{m}_g$ = 45.9 lb air/hr
$\dot{m}_s$ = 240 lb beads/hr
d = 329µ (1.079x10^{-3}ft)
D = 0.51 inches
T_o = 79°F
L = 36 inches

Project D-1

Coal Particle and Catalyst Characteristics for Hydrogenation Evaluation and Testing

Faculty Advisor: R.E. Wood
Graduate Student: J.M. Lytle

Introduction

This effort is related to the effects of coal particle size and temperature on the rate of coal hydrogenation in a coiled tube reactor and also a microreactor. The existing hydrogenation equipment was used with OCR (Office of Coal Research) Project, FE(49-18)-1200 and with ERDA-DOE Project, FE(49-18)-2006. The reaction vessel consists of a series of coiled tubes, each approximately 20 ft long and may be divided into two zones, preheater and reactor. The preheater consists of two coils each 20 ft long and 3/16 inch ID. The reactor consists of 1 to 4 coils, 20 ft long and 1/4 inch ID.

The residence time of coal and residual solids is measured in the reaction vessel of the coiled tube reactor using powdered iron as a tracer. The detection device consists of a coil of copper wire placed coaxially with the reactor tubing such that the ID of the copper coil is the same as that of the tubing. For residence time detection and measurement, one coil is placed at the beginning of the preheat section and a second at the end of the reactor.

The microreactor is a small batch reactor which may be heated rapidly to reaction temperature by a flame and cooled by water quench. Reactions normally may be considered nearly isothermal. The small size of the reactor also makes it convenient to weigh the whole system on a 5 place balance. This device will be used to study coal characteristics and coal-catalyst interactions.

Project Status

Tables 1-4 show data from the coiled tube reactor taken at various coal particle sizes and temperatures. The terms VM and FC represent volatile matter and fixed carbon, respectively.[1] In a given sample of coal the mass of volatile matter at a given time in the reactor is designated $(VM)_t$ and $(FC)_t$ for fixed carbon. The term

$$\frac{1-(VM)t}{(VM)_o}$$

where $(VM)_o$ is volatile matter at time 0, represents the fraction of volatile matter which becomes associated with the vapor phase or becomes toluene soluable at time, t. The total conversion is 1 minus the ratio of the moisture ash free (MAF) char (toluene insoluable residue) at time, t, and the MAF coal at time = 0. The residence time is the time the coal spends in the reactor at reaction conditions. The pressure is held at 123 atmospheres.

The following equation of Wiser et al.[2] was used to curve fit the data in Tables 1-4:

$$\frac{dx}{dt} = k\ (a-x)^n \qquad (1)$$

where x represents fractional conversion, k is the temperature dependent Arrhenius constant, a is the upper limit for x, t is the time and n is the reaction order. The integrated form of Eq (1) is

$$kt = \frac{a^{1-n}-(a-x)^{1-n}}{1-n} \qquad (2)$$

where x=0 at t=0. The fractions of total matter, volatile matter and fixed carbon converted are represented by X_c, X_{VM} and X_{FC}, respectively. Then

$$X_{VM} = \frac{1-(VM)_t}{(VM)_o}$$

and

$$X_{FC} = \frac{1-(FC)_t}{(FC)_o}$$

Eighteen curves, six each of X_c vs. time, X_{VM} vs. time and X_{FC} vs. time, have been calculated using Eq (2) and fit to the data of Tables 1-4. Temperatures range from 471 to 504°C and particle sizes from 105×10^{-6} to 364×10^{-6} meters. The values for a, k and n of Eq (2) are given for each curve in Table 5. These constants are calculated by choosing the maximum correlation coefficient over a range of values for a and n with the stipulation that x=0 at t=0. The 95% confidence limits for these curves are shown in Figures 1-6 and in Tables 1-4. To avoid confusion the actual curves are not drawn.

Significant separation with respect to particle size can be seen in the data at the 95% confidence level. (Figures 1-3). The separation is most apparent in FC (Figure 3) and least in VM (Figure 2). The VM evolution is dependent on but lags behind the heating rate such that the coal never reaches the temperature of the walls of the heating vessel. In a coke oven operation it takes about 18 hours to heat a 40 cm thick coal bed when heated from two sides.[3,4] Significant gas evolution takes place until the coal bed is completely heated. Even with very rapid heating rates, devolatilization correlates with the heating rate. Anthony et al. have devolatilized coal by heating to 900°C at a very rapid rate (750°C per sec).[5] The devolatilization rate levels off at about 1.2 sec as the sample temperature approaches 900°C. Therefore the devolatilization rate for a bituminous coal may be closely related to the heating rate.

The evolution of total volatile matter in the Clear Creek coal sample is a function of temperature (Figure 7). At 493°C the value of X_{VM} is about 0.6. Figure 2 shows little separation to that point. It takes 15 to 30 sec to travel the distance (10 meters) in the reactor tube which has an increasing temperature gradient. Generally large particles take longer than small particles. This causes some separation to become apparent even at $X_{VM} = 0.5$ as shown in Figure 2. The rate of change of X_{FC} as a function of time is dependent on the rate of hydrogenation. That this rate is particle size dependent implies that there is a physical rate controlling mechanism, i.e., heat transfer and/or diffusion. Because the two effects (heat transfer and diffusion) are dependent on both particle size and temperature, it is impossible to separate them mathematically or in a way in which they can be measured. The emperical expression for this dependence is

$$P = P_o + (0.97 + 0.118\ P_o^{-0.9})\ X_{FC}^{(0.71 + 0.011\ P_o^{-2})} \qquad (3)$$

where P is the actual average particle diameter and P_o is the initial average particle diameter (Figure 8, particle sizes are designated P_o).

For diffusion of hydrogen into the coal particle, the flux per unit surface area, N_H, is

$$N_H = -D_{H_2,C} \frac{dC_H}{dZ} \qquad (4)$$

where $D_{H_2,C}$ is the diffusivity of hydrogen into coal, C_H is the concentration of H_2 at some point in the coal particle and Z is the thickness of the concentration gradient.

Integrating Eq (4) and multiplying both sides by the outer surface area per unit mass, S, yields

$$N_H = \frac{D_{H,C} S \Delta C_H}{Z} \qquad (5)$$

The surface area per unit mass is dependent on the particle size, assuming spherical particles

$$S = 4\pi r^2 n \qquad (6)$$

where n is the number of particles per unit mass and r is the radius of the particles.

$$n = \frac{1}{\rho V} \qquad (7)$$

where $\rho = 1.3$ g/cm^3 and $V = 4/3\pi r^3$ is the average volume of the particles. Then Eq (6) becomes

$$S = \frac{3}{\rho r} \qquad (8)$$

and Eq (5) becomes

$$N_H S = \frac{3 D_{H,C} \Delta C_H}{\rho r Z} = \frac{6 D_{H,C} \Delta C_H}{\rho P Z} \qquad (9)$$

From Eq (9) the rate of hydrogen diffusion into the coal per unit mass is inversely proportional to the diameter, P, of the coal particles. Combined with Eq (3), Eq (9) becomes

$$N_H S = \frac{6\ D_{H,C} \Delta C_H}{\rho Z \left[P_o + (0.97 + 0.118\ P_o{}^{-0.9}) X_{FC}{}^{(0.71 + 0.011\ P_o{}^{-2})}\right]} \qquad (10)$$

The ρ, $D_{H,C}$ Z and ΔC_H may also be functions of X_{FC}. With the exception of ρ, the functionalities of the variables are much more difficult to determine. If diffusion is rate controlling, then $N_{H,S}$ will be proportional to dX_{FC}/dt and inversely proportional to P. The zero conversion level is the only condition in which there is a high degree of confidence in this calculation.

Figure 9 shows the reaction rate vs. the inverse of the particle size. Only a qualitative explanation of these curves is justified. The dependence of the rate equation on a diffusion and a concentration term is approximated by a resistance equation

$$\frac{1}{R} = \frac{1}{N_H S} + \frac{1}{K} \qquad (11)$$

where R is the rate, dX_{FC}/dt, and K is the chemical rate dependence. If $N_H S$ is small with respect to K, then $R \approx N_H S$ and the rate will be dependent on P^{-1}. If K is small with respect to $N_H S$, then $R \approx K$ and chemical rate control will become apparent. This occurs when the particle is very small and has a large surface area allowing the rapid diffusion of hydrogen. Thus dX_{FC}/dt is independent of particle size, causing the curve (Figure 9) to level off at smaller particle sizes. This is observed to a conversion level of 0.04. Leveling off of the curve may also occur at larger particle sizes. This would be caused by the greater effect of heat transfer within the particle. Extrapolation of the curves of Figure 9 shows this effect up to a 0.3 conversion level.

Future Work

Work will continue on developing a theory to explain Figures 4-6. The dependences of a and n on temperature will be investigated.

References

1. "Methods of Analyzing and Testing Coal and Coke," Bureau of Mines, Office of Coal Research, U.S. Dept. of the Interior, Bulletin 638, Washington, D.C., 1967.

2. W.H. Wiser, G.R. Hill and N.J. Kertamus, *Ind. Eng. Chem., Prod. Res. Develop.*, *6*, 133-138 (1967).

3. B.K. Mazundar and N.N. Chatterjee, *Fuel*, *52*, 11 (1973).

4. P.J. Wilson and J.H. Wells, "Coal, Coke and Coal Chemicals," McGraw-Hill, New York, N.Y., 1950.

5. D.B. Anthony, J.B. Howard, H.C. Hottel and H.P. Meissner, *Fuel*, *55*, 121 (1976).

Table 1. Clear Creek, Utah Coal at 100-200 mesh (average particle size 105 x 10^{-6} meters) processed in the coiled tube reactor at 493°C.

Run #	Residence Time, sec	Total Fractional Conversion	$\frac{1-(VM)_t}{(VM)_o}$	$\frac{1-(FC)_t}{(FC)_o}$
51	297	0.865	0.866	0.730
52	185	0.850	0.856	0.717
66	20	0.551	0.603	0.369
71	64	0.748	0.782	0.598
76	20	0.408	0.522	0.377

Table 2. Clear Creek, Utah Coal at 60-100 mesh (average particle size 195 x 10^{-6} meters) processed in the coiled tube reactor at 493°C.

Run #	Residence Time, sec	Total Fractional Conversion	$\frac{1-(VM)_t}{(VM)_o}$	$\frac{1-(FC)_t}{(FC)_o}$
24	211	0.838	0.801	0.718
25	172	0.832	0.812	0.686
29	81	0.719	0.712	0.570
55	211	0.815	0.837	0.686
56	96	0.777	0.814	0.638
60	239	0.829	0.827	0.735
65	20	0.382	0.502	0.200
72	26	0.438	0.560	0.241
73	19	0.447	0.578	0.238
87	30	0.525	0.587	0.446
88	22	0.374	0.485	0.232
91	6	0.137	0.299	0.155

Table 3. Clear Creek, Utah Coal at 40-60 mesh (average particle size 364 x 10^{-6} meters) processed in the coiled tube reactor at 493°C.

Run #	Residence Time, sec	Total Fractional Conversion	$\frac{1-(VM)_t}{(VM)_o}$	$\frac{1-(FC)_t}{(FC)_o}$
22	125	0.615	0.701	0.463
36	225	0.781	0.823	0.682
37	128	0.665	0.753	0.522
57	54	0.463	0.594	0.302
58	72	0.510	0.656	0.324
61	485	0.862	0.866	0.802
62	156	0.710	0.782	0.597
63	173	0.737	0.802	0.591
70	32	0.374	0.483	0.207
86	33	0.417	0.490	0.316
89	27	0.367	0.422	0.306
90	13	0.264	0.350	0.221

Table 4. Clear Creek, Utah Coal at 40-60 mesh (average particle size 364 x 10^{-6}m) processed in the coiled tube reactor.

Run #	Temp °C	Residence Time, sec	Total Fractional Conversion	$\frac{1-(VM)_t}{(VM)_o}$	$\frac{1-(FC)_t}{(FC)_o}$
41	471	97	0.508	0.586	0.387
47	471	95	0.492	0.560	0.363
48	471	178	0.709	0.736	0.643
69	471	57	0.298	0.368	0.184
32	482	69	0.473	0.588	0.362
33	482	234	0.793	0.806	0.714
34	482	74	0.451	0.55	0.311
38	482	71	0.433	0.597	0.250
39	482	111	0.580	0.677	0.458
40	482	175	0.728	0.776	0.644
68	482	52	0.370	0.449	0.229
43	504	157	0.754	0.831	0.624
45	504	436	0.832	0.876	0.735
50	504	176	0.747	0.779	0.678
67	504	38	0.525	0.590	0.401

Table 5. The mathematically optimum values of a, n and k for 18 curves calculated by the data of Tables 1-4 and the equation, $kt = \frac{a^{1-n} - (a-x)^{1-n}}{1-n}$

Particle Size (µ)		105	195	364	364	364	364
Temperature °C		493	493	493	471	482	504
a	conv	0.88	0.91	0.93	0.71	0.89	0.86
	VM	0.88	0.89	0.89	0.74	0.83	0.91
	FC	0.74	0.84	0.92	0.65	0.72	0.74
n	conv	1.56	2.01	1.77	0.34	1.06	1.61
	VM	1.69	2.32	1.63	0.52	1.04	1.84
	FC	1.39	1.96	1.74	0.01	0.39	1.13
k	conv	0.05716	0.05477	0.01823	0.00676	0.01020	0.02893
	VM	0.08924	0.12614	0.03062	0.00938	0.01646	0.04352
	FC	0.04296	0.02997	0.01039	0.00374	0.00553	0.01666

Figure 1. Residence Time vs. X_c for Clear Creek, Utah coal processed in the coiled tube reactor at 493°C, 123 atm H_2 press. and with 6.25% $ZnCl_2$ at various coal particle sizes.

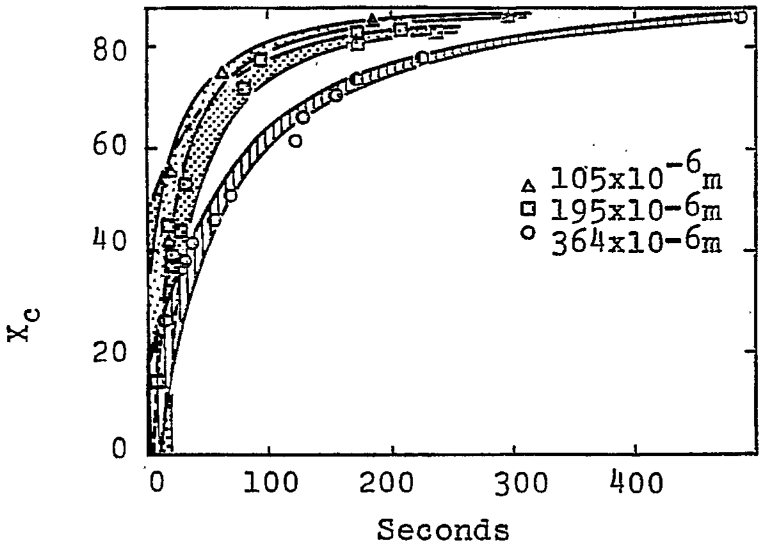

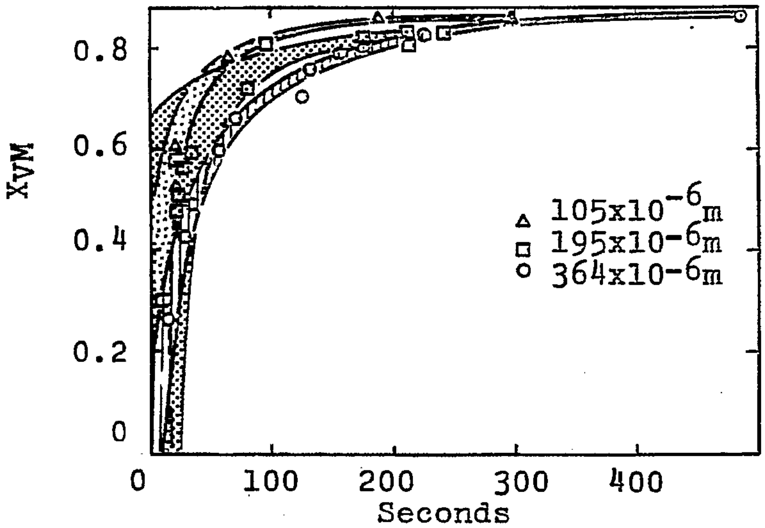

Figure 2. Residence time vs. X_{VM} for Clear Creek, Utah coal processed in the coiled tube reactor at 493°C, 123 atm H_2 press. and with 6.25% $ZnCl_2$ at various coal particle sizes.

Figure 3. Residence Time vs. X_{FC} for Clear Creek, Utah coal processed in the coiled tube reactor at 493°C, 123 atm H_2 Press. and with 6.25% $ZnCl_2$ at various coal particle sizes.

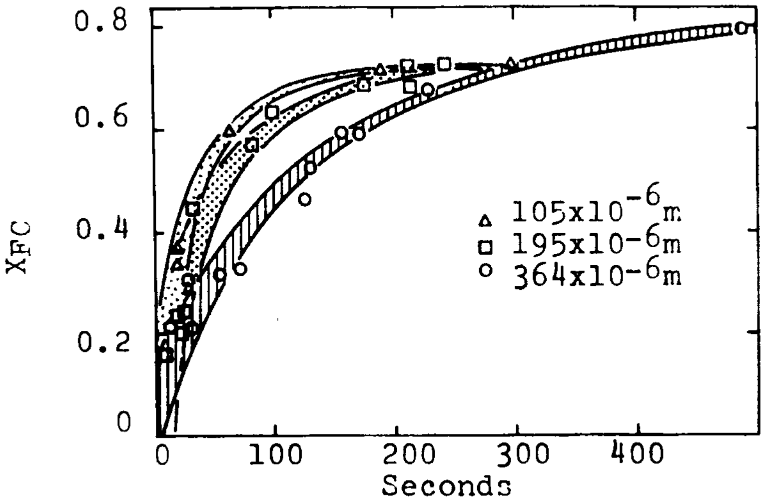

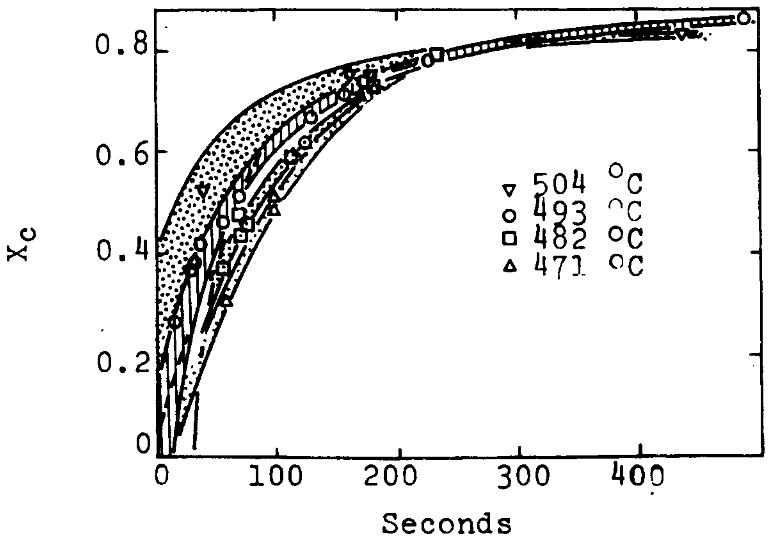

Figure 4. Residence time vs. X_c for Clear Creek, Utah coal processed in the coiled tube reactor at 123 atm H_2 press, 364×10^{-6} m coal particle size and with 6.25% $ZnCl_2$ at various temperatures.

Figure 5. Residence time vs. X_{VM} for Clear Creek, Utah coal processed in the coiled tube reactor at 123 atm H_2 press, 364×10^{-6}m coal particle size and with 6.25% $ZnCl_2$ at various temp.

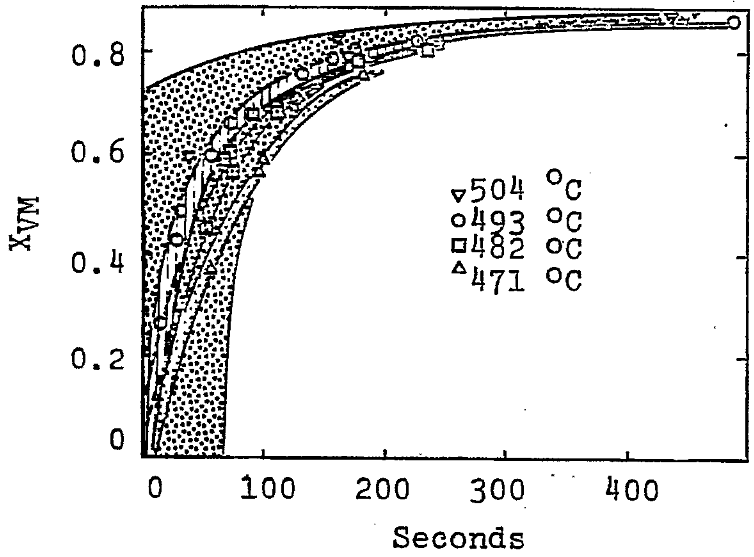

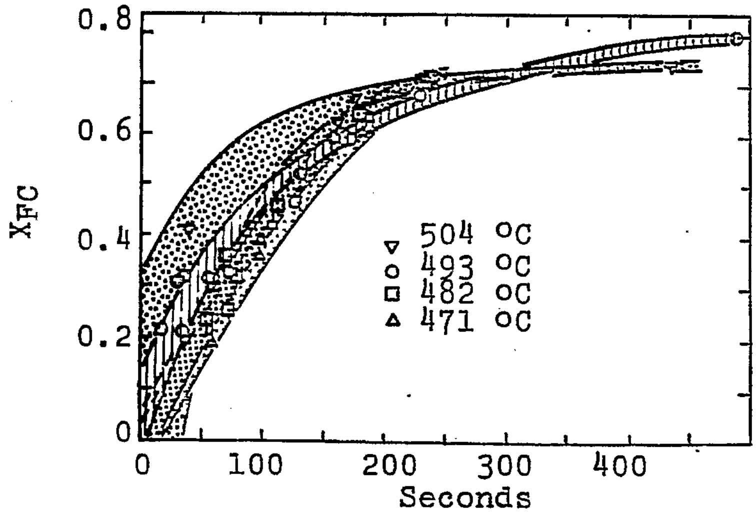

Figure 6. Residence time vs. X_{FC} for Clear Creek, Utah coal processed in the coiled tube reactor at 123 atm H_2 press, 364×10^{-6}m coal particle size and with 6.25% $ZnCl_2$ at various temperatures.

Figure 7. X_{VM} vs. temperature for Clear Creek, Utah coal with 6.25% $ZnCl_2$ on a MAF coal basis run in a std. volatile matter furnace for 7 min.

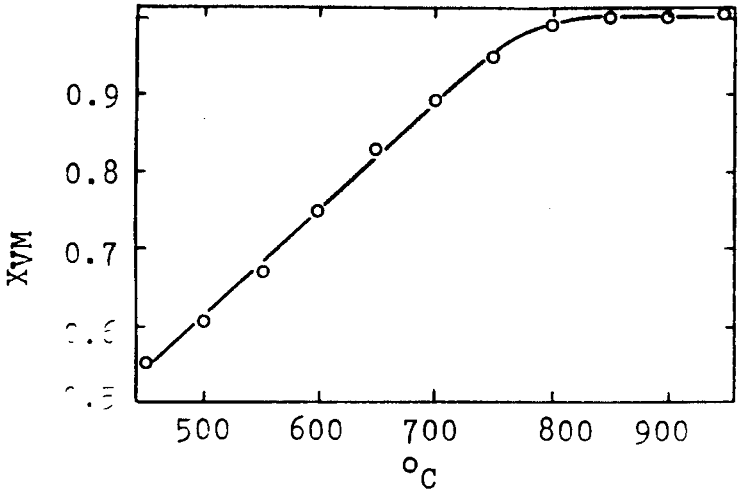

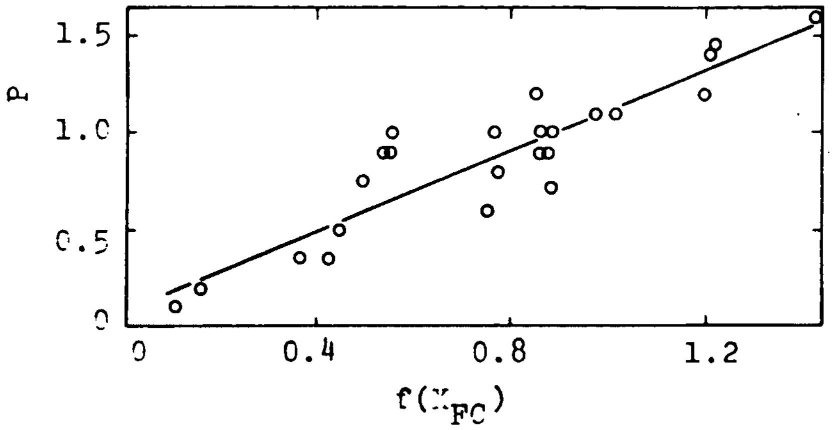

Figure 8. Particle size at any given X_{FC} in millimeters vs. $f(X_{FC}) = P_o+(0.97\pm 0.118/P_o^{0.9})X_{FC}^{(0.71+0.011/P_o^2)}$ The line is calculated from microscopic particle size measurements.

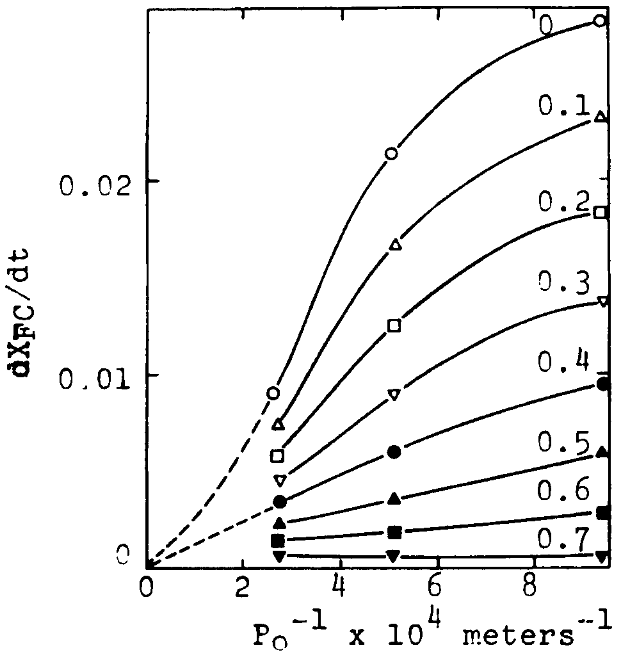

Figure 9. Reaction rate vs. the inverse of the initial particle size for various X_{FC} values.

Project D-1

Coal Particle and Catalyst Characteristics for Hydrogenation Evaluation and Testing

Faculty Advisor: R.E. Wood
Graduate Student: R. Jensen

Introduction

The mechanism of coal hydrogenation will be studied using $ZnCl_2$ as a catalyst and a small pressurized reactor, called a microreactor. This work will be a continuation of previous studies sited in a paper by D.P. Mobley et al.[1] The same model compounds will be studied using the optimum conditions of the University of Utah's coal hydrogenation system. These compounds represent various connecting groups found in coal and will be subjected to different temperatures, catalyst concentration and reaction times. The reaction products will be analyzed by gas chromatography and compared to proposed products from dealkylation of the model compounds, yielding reaction mechanism information.

Project Status

Three microreactors have been fabricated. A chart recorder and some pressure gauges, valves and fittings have been acquired. Preliminary chemistry of model compounds toward dealkylation reactions has been studied, and the gas chromatograph has been standardized.

Future Work

Reaction runs will be made with gas chromatographic analysis of the products. It is hoped that these studies will illuminate the reaction mechanisms.

References

1. D.P. Mobley, S. Salim, K.I. Tanner, N.D. Taylor and A.T. Bell, Preprints, Div. of Fuel Chemistry, American Chemical Society, Miami, Florida, Sept 1978, Vol 25 No. 4.

Project D-2

The Effect of Structure on Coal Reactivity

Structure of Coal Asphaltenes

Faculty Advisor: D.M. Bodily
Graduate Student: D. Roylance

Introduction

Asphaltenes have been thought by many investigators to be intermediates in the stepwise hydrogenation of coal to produce hexane-soluble oils. Recent reports have shown that coal can be liquified at very short reaction times and that asphaltenes and oils are produced by parallel reactions that can be interconverted by bond cleavage and polymerization reactions. Work in this laboratory (Project B-4) has shown that asphaltenes and oils from catalytic hydrogenation of coal are similar in structure, the major difference being size. Hexane-soluble oils appear to be composed of structural units comprised of condensed aromatic ring systems with alkyl groups and hydroaromatic rings attached. Asphaltenes appear to be polymers of these basic structural units. The nature of the bonds which hold these units together is of interest in this research.

Asphaltenes separated from the heavy oil from coal hydrogenation have been reacted by two processes. Catalytic dehydrogenation with Pd catalyst was used to react hydroaromatic structures. Reaction with HCl was used to separate the asphaltene into acid/neutral and base fractions.

Project Status

Results from structural analysis calculations are shown in Table 1. Molecular weights are shown in Table 2. The dehydrogenated asphaltene fractions show an increased fractional carbon aromaticity and decreased alkyl substitution on aromatic rings. The results are consistent with the dehydrogenation of hydroaromatic rings expected from the Pd catalyzed reaction. Considerable hydroaromaticity exists in the asphaltenes.

Treatment of the asphaltene with HCl results in separation into an acidic and neutral fraction and a basic fraction. The relative yields of the two fractions is different from that observed in asphaltenes produced in other processes. Separation and structural characterization of the acidic and basic compounds are complicated by their polarity.

Future Work

Mr. Roylance has completed the requirements for the MS degree and written a thesis on this topic. No further work is planned at this time.

Table 1

Structural Parameters from HNMR for Bulk Fractions FA and FD

Ve(ml.)		Ho/H+1	Fa	σ_T	σ_{al}	σ_o	Ca	Cp	Hau/Ca	M(us)
400	FA1	3.191	0.5576	0.5609	0.3507	0.2102	14.3541	10.1771	0.7090	355.61
470	FA2	2.955	0.5943	0.4203	0.2612	0.1591	7.8288	6.9144	0.8832	190.27
530	FA3	1.715	0.6410	0.4669	0.3601	0.1068	7.3800	6.690	0.9065	161.40
600	FA4	1.693	0.7505	0.2953	0.2733	0.0220	13.6923	9.8461	0.7191	238.49
680	FA5	1.711	0.8072	0.2672	0.2424	0.0148	40.107	23.054	0.5748	637.73
345	FD1	5.114	0.6404	0.4083	0.2435	0.1648	61.100	27.55	0.4509	1302.44
450	FD2	3.903	0.6490	0.3519	0.2180	0.1399	22.124	14.062	0.6356	473.50
535	FD3	2.935	0.6932	0.2980	0.2108	0.0872	13.787	9.794	0.7176	271.89
630	FD4	1.802	0.9208	0.0789	0.0675	0.114	14.670	10.335	0.7045	205.04
680	FD5	1.313	0.9320	0.0790	0.0790	0.	14.771	10.385	0.7031	201.90
835	FD6	6.05	0.7236	0.2178	0.1026	0.1152	24.814	15.402	0.6207	472.05
2000	FD7	5.69	0.4214	0.4816	0.2794	0.2022	8.1411	7.071	0.8685	281.61

Table 1 (Continued)

Structural Parameters from HNMR for Bulk Fractions FAC and FB

Ve(ml.)		Ho/H+1	Fa	σ_T	σ_{al}	σ_o	Ca	Cp	Hau/Ca	M(us)
400	FAC1	4.398	0.6040	0.1874	0.1712	0.0162	8.1345	7.067	0.8688	179.68
485	FAC2	3.333	0.5611	0.4087	0.2673	0.1414	7.903	6.951	0.8796	201.37
570	FAC3	4.516	0.4513	0.5614	0.3911	0.1703	15.789	10.894	0.690	493.30
600	FAC4	4.866	0.4675	0.4865	0.3583	0.1282	19.206	12.603	0.6562	570.42
780	FAC5	4.162	0.6252	0.3540	0.2098	0.1442	15.865	10.933	0.6891	356.32
2000	FAC6	17.22	0.4247	0.5882	0.1263	0.4619	21.818	13.909	0.6375	793.84
500	FB1	3.335	0.5727	0.4731	0.3542	0.1189	22.455	14.214	0.6330	539.10
695	FB2	3.0	0.5720	0.4197	0.3368	0.0829	12.381	9.19	0.7423	296.09
760	FB3	1.673	0.7899	0.3789	0.3470	0.0319	14.191	10.100	0.7114	269.80
820	FB4	1.890	0.8362	0.2263	0.1481	0.0782	15.053	10.527	0.6993	243.20
2000	FB5	3.588	0.6085	0.5090	0.2422	0.2668	12.371	9.185	0.7425	303.92

Table 2

Molecular Weight (MW) Calculations

	M W
FA1	559.9
FA2	292.7
FA3	264.3
FA4	292.9
FA5	201.2
FD1	475.8
FD2	453.5
FD3	316.4
FD4	181.9
FD5	173.0
FD6	315.6
FD7	316.5
FAC1	647.7
FAC2	446.6
FAC3	349.8
FAC4	310.0
FAC5	335.6
FAC6	200.2
FB1	278.4
FB2	398.0
FB3	310.4
FB4	307.3
FB5	277.7

Project D-4

Pyrolytic Studies and Separation and Characterization of Coal-Derived Liquids

The Separation and Characterization of Coal-Derived Liquids

Faculty Advisor: R.R. Beishline

Introduction

This project deals with the investigation of promising methods for analyzing and identifying the lighter fraction of coal hydrogenation liquids. A spinning band (SB) distillation column (> 200 theoretical plates at atm press) is being used to determine whether fractionation can separate pure components directly from complex coal-derived liquids. Also SB distillation in combination with preparative gas chromatography (PGC) is being tested.

SB fractionation of crude material boiling up to 150°C (atm) did not give distillates consisting of pure components, but did effectively cut the pot charges into smaller less complex fractions.

Using SB distillation in combination with PGC, the components in an 80-100°C (atm press) coal liquid fraction have been separated and isolated, and compounds representing about 70 volume % of the fraction have been spectroscopically identified (MS, IR, NMR). (Identification by GC-MS is more time economical.)

The development of a scheme for the analysis of the ambient - 80°C (A-80) fraction of coal liquids has been completed.

Project Status

The development of a procedure for the analysis of the ambient - 80°C (A-80) fraction of coal liquids was completed last quarter and is briefly outlined, in total, here.

The crude coal liquids are a two phase organic-water mixture. This mixture is distilled (water and hydrocarbons co-distill) until the water has been removed, and then further distilled until the head temperature reaches 150°C (crude distillate). The aqueous and organic phases of the crude distillate are separated, and the organic phase dried over anhydrous magnesium sulfate. This dried crude distillate is fractionated through a spinning band (SB) distillation column (200:1 reflux ratio, > 200 theoretical plates) and collected in a cooled receiver (dry ice acetone) up to 80°C (A-80 fraction). Triplicate SB fractionations of a representative crude distillate (25 ml pot charge) gave 1.28 ± 0.09 ml of distillate (a standard deviation of 7% in the volume of distillate). The representative crude distillate was made by mixing the dried crude distillates obtained from the hydrogenation of several different Utah coals. The A-80 fraction was analyzed with a gas chromatograph coupled to an electronic integrator (1/8" x 6' stainless steel column, carbopack C/0.19% picric acid packing, 60 ml/ min He, 55° to 120°C programmed at 1.5°/min). The average standard deviation in the integrated area percents for triplicate GC analysis of a single A-80 fraction is 0.60 percent. This represents the average combined error in the reproducibility of sample injection, column resolution, detector response and electronic integration.

The identity of the individual GC peaks has been established by GC-MS (all by empirical formula and many by specific isomer). The identification work was reported in the Jan-March, 1978 Quarterly Progress Report.

Future Work

The separation of the A-80 coal liquid fraction on a capillary GC-MS has been scheduled at the Flammability Research Center at the University of Utah. When this work is completed, it will be reported. With this exception, the proposed work on this project has been completed, and Project D-4-I has been terminated.

Project D-4

A Pyrolysis-Gas Chromatography Study of Coals and Related Model Compounds

Faculty Advisor: R.R. Beishline

Introduction

This project deals with the pyrolysis and hydrogenation of coal and coal-related model compounds both in the presence and absence of catalysts.

Since coal hydrogenations are normally carried out at thermolytic temperatures, reactions other than hydrogenation likely occur concurrently, e.g., pyrolysis and reactions that can be catalytically initiated at subthermolytic temperatures and that would proceed at accelerated rates at thermolytic temperatures. A knowledge of these latter reactions is a necessary background to the understanding of the hydrogenation chemistry. To elucidate some of this background, the subthermolytic (165°C) zinc chloride-catalyzed decomposition of the model compound 1,2-dihydronaphthalene (1,2-DHN) has been studied.

The decomposition occurs by a mechanism in which hydrated zinc chloride donates a proton to the double bond of 1,2-DHN to form a carbonium ion. This carbonium ion adds to 1,2-DHN to give two dimers and abstracts hydride from 1,2-DHN to produce tetralin and naphthalene.

A study of the pyrolysis of 1,2-DHN has been initiated, and preliminary kinetic results suggest that the following scheme of simultaneous first and second order reactions is operative.

$$\text{1,2-DHN} \longrightarrow \text{naphthalene} + H_2 \qquad \text{(I)}$$

$$2(\text{1,2-DHN}) \longrightarrow \text{tetralin} + \text{naphthalene} \qquad \text{(II)}$$

The 1,2-DHN is an intermediate in the hydrolique faction of coal when tetralin is used as the hydrogen donor solvent.[1] Reactions (I) and (II) are thus part of the overall hydrogen transfer scheme

$$\text{coal} + \text{tetralin} \longrightarrow \text{hydrogenated coal} + \text{naphthalene}$$

and are of considerable interest.

Project Status

Additional kinetic data for Reactions (I) and (II) have been collected for determining activation energies and working out a scheme to kinetically handle side reactions. A report of these results will be made when collection of the data is completed.

Past work has shown that at higher temperatures (400°C), 1,2-DHN can dehydrogenate a dihydroaromatic ring to an aromatic ring, the 1,2-DHN being hydrogenated to tetralin. This suggests the interesting and relevant question: Can 1,2-DHN dehydrogenate a tetrahydroaromatic ring to a dihydroaromatic ring? If this reaction were studied in the tetralin system, some tracer or labeling technique would be required since the products are identical to the reactants. Therefore, this reaction will be studied using 1,2-DHN and tetrahydrophenanthrene (THP) as the reactants. The THP has been synthesized according to Scheme I and its pyrolytic behavior evaluated. The pyrolytic evaluation was necessary to distinguish the thermal decomposition of pure THP from the reaction of 1,2-DHN with THP. The results of the pyrolytic experiments are summarized in Table 1. Most of the pyrolysis products have not been identified and are tabulated by retention time only. These data (Table 1) indicate the reaction of 1,2-DHN with THP can be conveniently studied in the 400-450°C range, since pure THP decomposes only to the extent of 2-7% (20 min) in that range.

The chemistry of 1,2 and 3,4-dihydrophenanthrene (1,2 and 3,4-DHP) will also be investigated to determine whether it is analogous to that of 1,2-DHN. The synthesis of 1,2 and 3,4-DHP is now in progress.

Future Work

The kinetic study of Reactions (I) and (II) will be continued. A study of the reaction of 1,2-DHN with THP will be initiated, and work will continue on the synthesis of 1,2 and 3,4-DHP.

References

1. L.L. Anderson, D. Kang and W.H. Wiser, DOE Contract No. (49-18) - 2006, Quarterly Progress Report, Salt Lake City, Utah, July-Sept, 1977.
2. R.D. Haworth, _J. Chem. Soc._, 1129 (1932).
3. Org. Synthesis Coll. Vol. II, 499 (1955).
4. Org. Reactions, Vol. 2, 136-7 (1947).
5. Org. Reactions, Vol. 1, 156-81 (1947).

Scheme I

Ref

Naphthalene

↓ succinic anhydride $AlCl_3$ 2

4-keto-4-(1-naphthyl) butanoic acid
+
4-keto-4-(2-naphthyl) butanoic acid

↓ Zn (Hg) 3

4-(1-naphthyl) butanoic acid
+
4-(2-naphthyl) butanoic acid

↓ PCl_5 or $SOCl_2$ 4

4-(1-naphthyl) butanoyl chloride
+
4-(2-naphthyl) butanoyl chloride

↓ $SnCl_4$ 4

1-keto-1,2,3,4-tetrahydrophenanthrene
+
4-keto-1,2,3,4-tetrahydrophenanthrene

↓ Zn (Hg) 5

1,2,3,4-tetrahydrophenanthrene

Table 1. Preliminary GC Analysis[a] of Tetrahydrophenanthrene Pryolysis Products (20 min rctn time).

		Area % Compound in Reaction Products					
Product (ret time, min)	Control (rm temp)	300°C	350°C	400°C	450°C	500°C	550°C
2.07						0.08	4.22
2.77						0.48	8.65
3.05						0.25	3.32
3.59					0.26	4.28	11.86
4.86						0.31	0.98
5.96	0.14		0.39	0.93	1.78	2.82	1.13
8.43		0.17	0.56	0.68	1.34	10.00	6.35
11.42							0.93
16.28 Tetrahydrophenanthrene	96.94	99.73	97.24	98.09	93.15	67.40	--
18.56	2.92	0.10	--	--	--	--	--
25.87 Phenanthrene	--	--	1.71	0.28	3.43	14.29	62.46

[a] GC analysis conditions: 4' x 1/4" Cu column, 15% carbowax 20M on 80/100 mesh Chromosorb-P: 100 ml/min He; 210°C isothermal.

Hydrodesulfurization of Heavy Hydrocarbon Liquids in a Fluidized Bed Reactor with Hydrogen as the Continuous Phase

Faculty Advisor: A.G. Oblad
Graduate Student: Hsiang-Yun Kung

Introduction

Commercial hydrodesulfurization processes are operated mostly in fixed bed reactors. For fixed bed reactors, fine catalyst particles can not be used because of the excessive bed pressure drop; neither can fresh catalyst be added without reactor shut down. However, with a fluid bed reactor, it is possible to 1) operate at near isothermal conditions because of the radial and axial agitation induced by the bubbles, 2) maintain constant activity of the catalyst by continuous circulation of the spent or coked catalyst between the reactor and regenerator, 3) have an essentially constant yield and quality of the products from operating at a constant temperature and catalyst activity, 4) change the feed or product quality on a given feed by controlling the catalyst withdrawal rate which adjusts the equilibrium activity and 5) employ very small catalyst sizes for catalytic effectiveness.

Therefore, the objective of this study is to determine the feasibility of the vapor-phase fluidized bed hydrodesulfurization of commercial feedstocks such as straight run gas oil. The parameters are

Temperature:	400-450^{o}C
Pressure:	1000-1500 psig

The catalysts being studied, along with their physical properties have been given in the previous report. The catalyst (average particle size: 49 microns) was prepared by grinding a commercial cobalt-molybdate oxide supported on alumina and subsequently sulfiding the selected size fraction with H_2S for 2 to 4 hours at 300^{o}C, 20 psig.

Project Status

The minimum fluidization velocity, the most important constant of a fluidization system, was determined using the method of Kunii and Levenspiel.[1] The pressure drop across the taps (Figure 1), located below the bottom distributor plate and above the top solids retaining plate, was measured at operation conditions for various gas flow rates. The reactor was loaded with a known amount of catalyst and again the pressure drop was measured at different gas flow rates. The bed pressure drop was estimated by subtracting the value of the pressure drop across the bottom and top plates from the total pressure drop across the plates and the bed at the same gas rate.

Preliminary experiments have been carried out to determine the minimum fluidization velocities under high pressure and temperature. The data are given in Table 1 and plotted in Figures 2 and 3.

Several studies on gas-solid fluidized beds at atmospheric pressure have shown that the pressure drop in the fluidized state (ΔP) may differ from the buoyant weight of solids per unit area (ΔP_{eq}) depending on the bed diameter, bed depth/diameter ratio, gas velocity, nonuniformity in the structure of bed, type of distributor, etc. For the fluidization of glass beads with air at atmospheric pressure, Trivedi and Rice[2] observed that the ratio $\Delta P/\Delta P_{eq}$ ranged from 0.85 to 1.4 over the range of a bed depth/diameter ratio of 1.41 to 14.87 for two column diameters of 1.769 and 4.25 inches.

The pressure drop kept rising with increasing air velocity for deeper beds in the fluidized region. For a smaller range of a bed-depth/diameter ratio, Lewis et al.[3] reported the $\Delta P/\Delta P_{eq}$ ratio of 0.98 to 1.15 for 2.5 and 4.5 in. tube diameters. Lewis et al.[3], Trivedi and Rice[2] and Othmer[4] explain the case of shallow beds ($\Delta P/\Delta P_{eq}<1$) as a condition under which all the particles in the bed are not supported by the gas. The case of deeper beds ($\Delta P/\Delta P_{eq}>1$) is explained by 1) Johnstone et al.[5] as due to kinetic energy losses caused by the collision between particles, 2) Lewis et al.[3] as an indication of frictional drag (both gas and solid) on the walls of the unit, 3) Wilhelm and Kwauk[6] as due to electrostatic forces and 4) Trivedi et al.[2] as due to slugging and electrostatic forces. Mori[7] has also reported a wide deviation of ΔP compared to ΔP_{eq} for high pressure fluidized beds using glass beads and coal particles. For example, a $\Delta P/\Delta P_{eq}$ ratio of 2.03 has been reported compared with the theoretical value of 1.0 for fluidization of coal particles, 0.0363 cm average diameter, with CO_2 at 500 psig and 320°K .

Future Work

The measurement of the minimum fluidization velocity will be performed for various particle sizes at different operating conditions.

References

1. D. Kunii and O. Levenspiel, "Fluidization Engineering," John Wiley and Sons, Inc., New York, N.Y., 1969, p 74.

2. R.C. Trivedi and W.J. Rice, Chem. Eng. Progr., Symp. Ser., 62 (67), 57 (1966).

3. W.K. Lewis, E.R. Gilliland and W.C. Baur, Ind. Eng. Chem., 41, 1104 (1949).

4. D.F. Othmer, "Fluidization," Reinhold, New York, N.Y., 1956.

5. H.F. Johnstone and R. D. Roomey, Chem. Eng. Progr., 48, 220 (1952).

6. R.E. Wilhelm and M. Kwauk, Chem. Eng. Progr., 44, 201 (1948).

7. S. Mori, Ph.D. Thesis, University of Utah, Salt Lake City, Utah, 1973.

Table 1. Pressure Drop Across Bed at Different Gas Velocities Bed Conditions.

Particle: Sulfided Co-Mo-Al (Harshaw 0603)
Pressure: 1000 psig
Temperature: 425°C
Mean Diameter: 49 microns
Bed Weight: 63.3 g
Fixed Bed Height: 12.19 cm
Pressure Drop Equivalent to Bed Weight (ΔP_{eq}): 4.93 in. water
Fixed Bed Depth/Column Diameter: 4.8

H_2 Flow Rate std cc/sec	H_2 Velocity (cm/sec at reactor conditions)	ΔP Across Bed (inches water)	$\Delta P/\Delta P_{eq}$
9	0.067	0.5	0.101
12	0.089	1.6	0.325
11	0.081	2.5	0.507
19	0.141	4.1	0.832
23	0.170	5.4	1.095
35	0.259	7.0	1.420
45	0.333	8.8	1.785
44	0.326	10.0	2.028
57	0.422	11.7	2.373
60	0.444	13.4	2.718
72	0.533	15.0	3.043
73	0.540	15.5	3.144
79	0.585	16.4	3.327
86	0.636	16.0	3.245
109	0.807	16.0	3.245

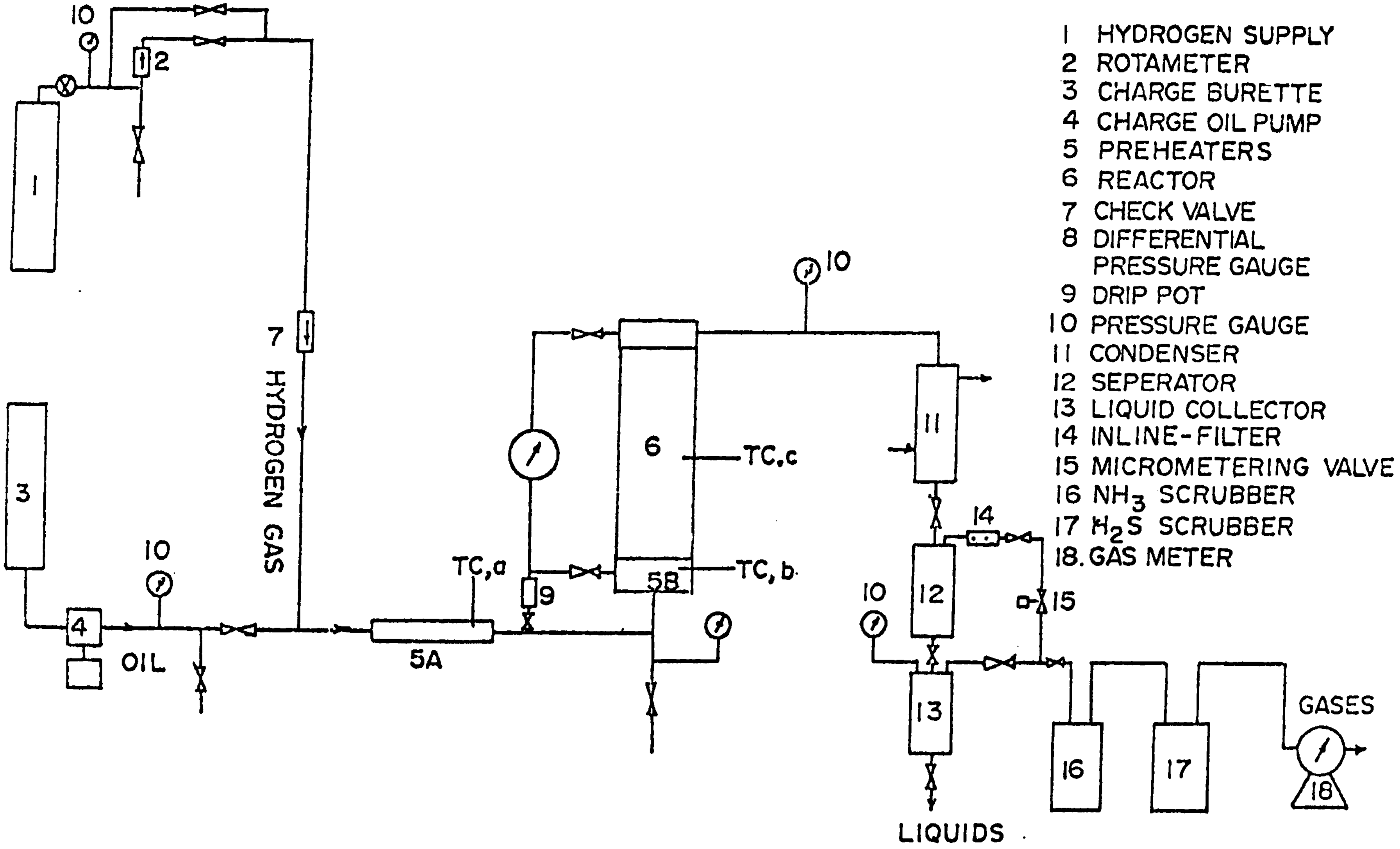

Figure 1.Flow Diagram of HDS Process

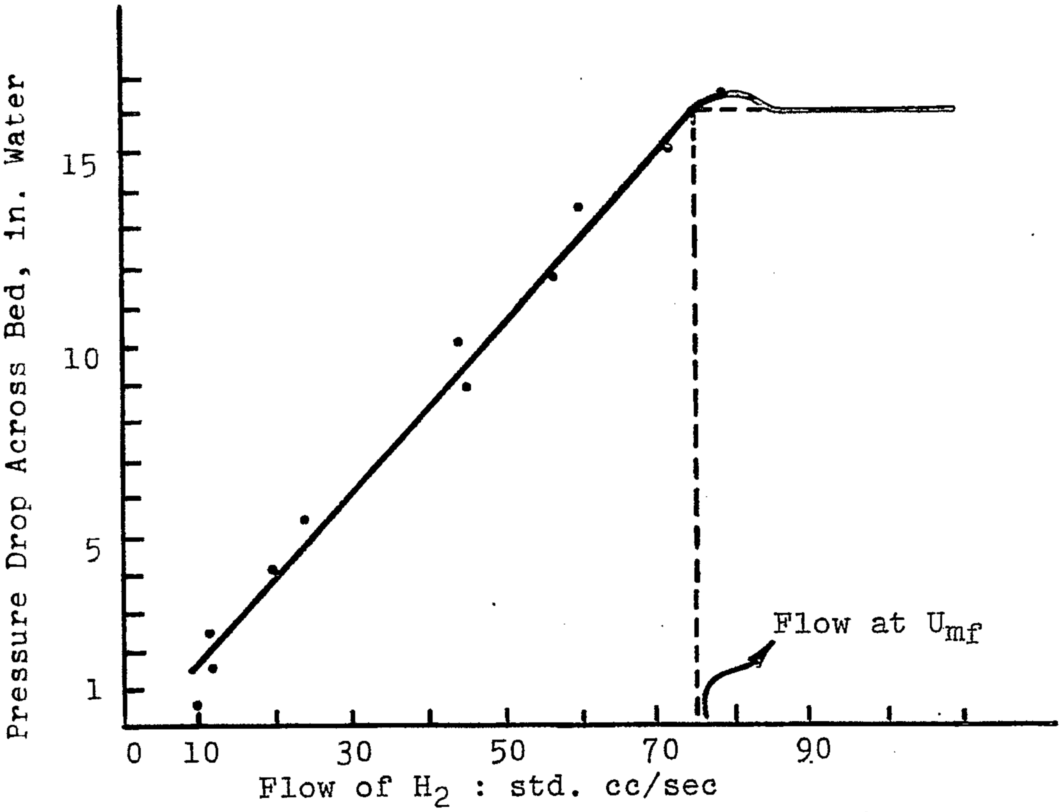

Figure 2. Bed Pressure Drop Vs. Gas Flow Rate.

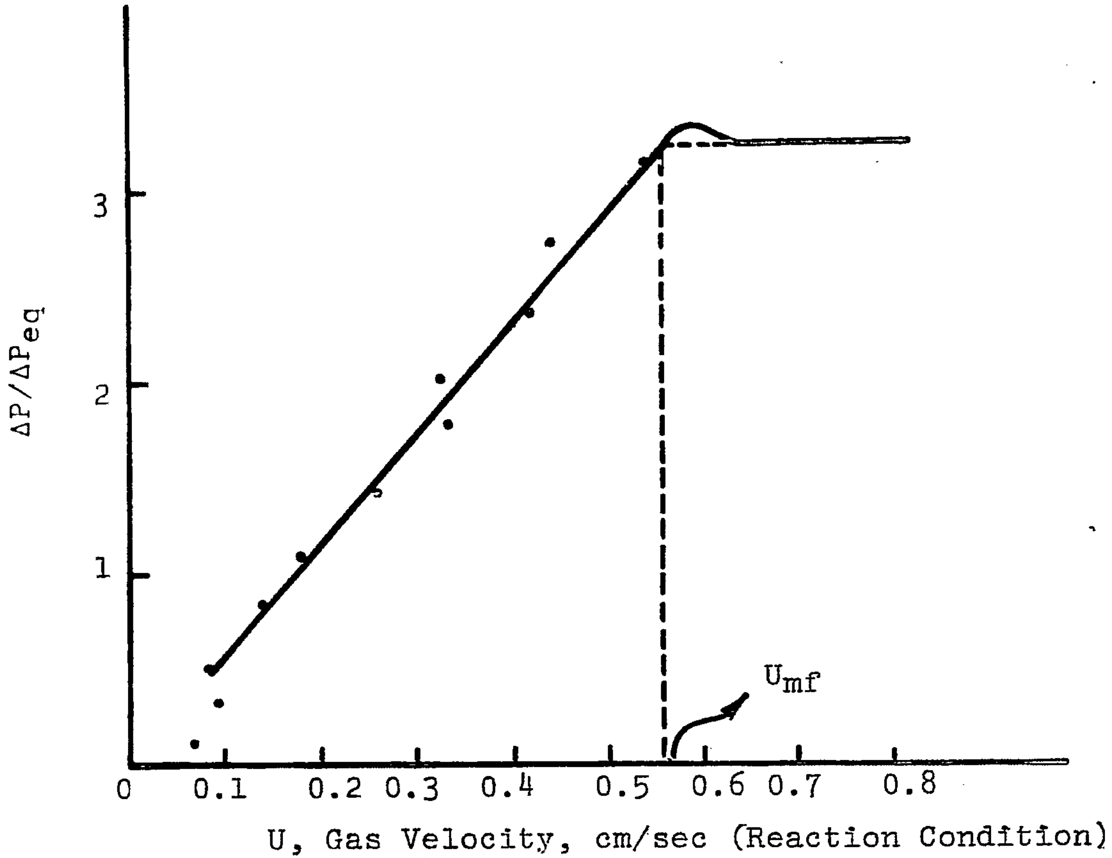

Figure 3. Ratio of Experimental Bed Pressure Drop to that Equivalent to the Bed Weight Vs. Hydrogen Velocity.

V. Conclusion

Twelve projects plus one supplemental project were active during the quarter. Projects A-6 and A-9 have not been initiated. Project B-3 has been completed. Students on Projects A-4, C-1 and D-2 have completed their studies. Other aspects of these projects will be initiated when students are available.

Reproduced by NTIS

National Technical Information Service
Springfield, VA 22161

This report was printed specifically for your order from nearly 3 million titles available in our collection.

For economy and efficiency, NTIS does not maintain stock of its vast collection of technical reports. Rather, most documents are custom reproduced for each order. Documents that are not in electronic format are reproduced from master archival copies and are the best possible reproductions available.

Occasionally, older master materials may reproduce portions of documents that are not fully legible. If you have questions concerning this document or any order you have placed with NTIS, please call our Customer Service Department at (703) 605-6050.

About NTIS

NTIS collects scientific, technical, engineering, and related business information – then organizes, maintains, and disseminates that information in a variety of formats – including electronic download, online access, CD-ROM, magnetic tape, diskette, multimedia, microfiche and paper.

The NTIS collection of nearly 3 million titles includes reports describing research conducted or sponsored by federal agencies and their contractors; statistical and business information; U.S. military publications; multimedia training products; computer software and electronic databases developed by federal agencies; and technical reports prepared by research organizations worldwide.

For more information about NTIS, visit our Web site at http://www.ntis.gov.

NTIS

Ensuring Permanent, Easy Access to U.S. Government Information Assets

SATISFACTION GUARANTEED

NTIS strives to provide quality products, reliable service, and fast delivery. Please contact us for a replacement within 30 days if the item you receive is defective or if we have made an error in filling your order.

- **E-mail: info@ntis.gov**
- **Phone: 1-888-584-8332 or (703)605-6050**

U.S. DEPARTMENT OF COMMERCE
Technology Administration
National Technical Information Service
Springfield, VA 22161 (703) 605-6000